

NPS ARCHIVE  
1966  
KIRBY, A.

AN APPLICATION OF VORTEX GENERATORS TO  
A SINGLE SLOTTED FLAP

by

Lt. A. <sup>lex</sup> G. Kirby Jr. USN

Lt. F. M. Graham USN

May 1964



PRINCETON UNIVERSITY  
DEPARTMENT OF  
AEROSPACE AND MECHANICAL SCIENCES

Thesis  
K49

Library  
U. S. Naval Postgraduate School  
Monterey, California



AN APPLICATION OF VORTEX GENERATORS TO  
A SINGLE SLOTTED FLAP

by

Lt. A. <sup>lex</sup>G. Kirby Jr. USN

Lt. F. M. Graham USN

May 1964

Submitted in partial fulfillment of the requirements  
for the Degree Of Master of Science in Engineering  
from Princeton University

NPS ARCHIVE  
1966  
KIRBY, A.

~~Thesis~~

~~K49~~

#### ACKNOWLEDGEMENT

The authors wish to express their appreciation to Mr. Thomas E. Sweeney for his ideas, guidance, and assistance throughout this investigation, and to the Hangar staff for their assistance in installing the required instrumentation and in performing the necessary maintenance to keep the aircraft flyable during this investigation.

The authors acknowledge with gratitude the opportunities for postgraduate education provided by the United States Navy.

Appreciation is also expressed to Mr. Marcus Knowlton and Mr. William James for their assistance during the wind tunnel phase of this investigation.

To Mrs. Geraldine Fudge we are indebted for her perseverance in typing this manuscript.



## TABLE OF CONTENTS

	Page
Summary.....	i
Introduction.....	1
List of Symbols.....	2
Specifications.....	3
Equipment.....	5
Aircraft.....	5
Wind Tunnel.....	5
Model Construction.....	7
Procedures.....	10
Introduction.....	10
Wind Tunnel.....	10
Flight Testing.....	13
Power Required.....	15
Results.....	17
Wind Tunnel.....	17
Flight Test.....	18
Discussion.....	20
Conclusions.....	25
References.....	27
Figures.....	28





# AN APPLICATION OF VORTEX GENERATORS TO

## A SINGLE SLOTTED FLAP

### SUMMARY

With the current interest in V/STOL aircraft, there have been various devices designed to improve the take-off and landing characteristics of an aircraft by delaying the flow separation in the presence of adverse pressure gradients. This report contains the results of an investigation to determine the effect of vortex generators mounted on a single slotted flap. This area of investigation is especially applicable to light and moderate weight aircraft as there is no complex mechanical equipment associated with these devices and the vortex generators represent a negligible increase in aircraft gross weight.

It was concluded that the cambered vortex generators were installed at too large an effective angle of attack and acted as spoilers at the zero and one-half flap settings, giving a reduction in the maximum lift coefficient and an increase in drag coefficient. At the full flap setting, the vortex generators gave a significant reduction in drag coefficient and power required for level flight. There was also a reduction in maximum lift coefficient, as a function of power required for level flight, for zero and half flap settings but an increase in maximum lift coefficient with full flaps. The application of vortex generators resulted in no adverse handling qualities or reduction in stability.

This investigation was conducted by Lt. A. G. Kirby and Lt. F. M. Graham, USN, at the James Forrestal Research Center of Princeton University during academic year 1963-1964 under the guidance of Mr. Thomas E. Sweeney, Senior Research Engineer, Department of Aerospace and Mechanical



Sciences, Princeton University, Princeton, New Jersey.



# AN APPLICATION OF VORTEX GENERATORS TO A SINGLE SLOTTED FLAP

## INTRODUCTION

With the current increased interest in V/STOL aircraft, there have been various efforts to increase the takeoff and landing performance of light and medium weight aircraft without the associated weight and complexity of suction devices to remove the boundary layer or high velocity jets of air to increase the energy content of the boundary layer in the presence of an adverse pressure gradient. Any modification to the aircraft should add a minimum of drag to the aircraft while providing a significant increase in maximum lift coefficient. This increase in lift coefficient would allow the aircraft to take off in a shorter ground roll or carry more payload for the same ground roll. The increase in lift coefficient would also allow for a decrease in approach speed with a subsequent decrease in landing roll.

This investigation was designed to study the idea of attaching vortex generators to the flaps of an aircraft in order to keep the flow attached to the flaps at high deflection angles. By installing vortex generators, the momentum of the free stream flow would be mixed with the boundary layer, increasing the energy content of the boundary layer and delaying the separation of the flow across the flaps. This delay of flow separation would give an increase in maximum lift coefficient.

This investigation was conducted by Lt. A. G. Kirby and Lt. F. M. Graham, USN under the guidance of Mr. Thomas E. Sweeney, Senior Research



Engineer, of the Department of Aerospace and Mechanical Sciences of  
Princeton University, Princeton, New Jersey.

This investigation was conducted during academic year 1963-1964.





## LIST OF SYMBOLS

## UPPER CASE

$C_L$	Lift Coefficient	- $L/qS$
$C_D$	Drag Coefficient	- $D/qS$
D	Drag	- pounds
L	Lift	- pounds
P	Pressure	- lbs./sq. ft.
R	Universal Gas Constant	- Sq. ft./sec <sup>2</sup> T <sup>0</sup>
T	Temperature	- Degrees Rankine
AR	Aspect Ratio	
S	Area	- sq. ft.

## LOWER CASE

e	Oswald Efficiency Factor	
q	Dynamic Pressure	- lbs./ft. <sup>2</sup>
$\nu$	Kinematic Viscosity	- ft. <sup>2</sup> / sec.
$\rho$	Density	- lbs. sec <sup>2</sup> / ft. <sup>4</sup>
$\delta$	Boundary Layer Thickness	- inches
$\delta_e$	Elevator Deflection	- degrees
$\delta_f$	Flap Deflection	- degrees



## NAVION SPECIFICATIONS

WING AREA (including flaps, ailerons, 19.8 sq. ft. of fuselage)	183.34 sq. ft.
SPAN	33.38 ft.
MAC	62.35 inches
Incidence of root	+2 <sup>0</sup>
Incidence of tip	-1 <sup>0</sup>
Aerodynamic Twist	2 <sup>0</sup> 31'
Geometric Twist	3 <sup>0</sup>
Root Section	NACA 4415R
Tip Section	NACA 6410R
Aspect Ratio	6.04
Taper Ratio	0.54
Dihedral	7.5 <sup>0</sup>
Root Chord	7.2 ft.
Tip Chord	3.92 ft.
Sweep of Leading Edge	3.0 <sup>0</sup>
VERTICAL TAIL	
Total Area (including 2.57 sq. ft. blanketed by fuselage and excluding 1.84 sq. ft. dorsal fin area)	12.93 sq. ft.
Stabilizer Area	6.87 sq. ft.
Rudder Area	6.06 sq. ft.
Root Section	Modified NACA 0013.2
Tip Section	Modified NACA 0012-64
Angle of Stabilizer to Fuselage	2 <sup>0</sup> nose left
Span	4.05 ft.



## HORIZONTAL TAIL

Total Area (including 2.37 sq. ft. covered by fuselage)	43.05 sq. ft.
Stabilizer Area	28.95 sq. ft.
Elevator Area	14.10 sq. ft.
Taper Ratio	0.67
Aspect Ratio	4.02
Section	NACA 0012
Span	13.18 ft.
MAC	3.34 ft.
Angle of Incidence	-3°

## GENERAL

Overall Length	27.25 ft.
Tail Length	16.88 ft.
Weight (full fuel and 8.5 qts. of oil)	2203 lbs.

## POWERPLANT

Continental E-185

185 H. P. at 2300RPM  
at 29" Hg M.A.P. at S.L.

## PROPELLER

HARTZEL

Activity Factor	100
Diameter	86 inches
Pitch at 0.75 radius	26.5°



## EQUIPMENT

## AIRCRAFT

The aircraft used in this investigation was a Ryan Navion, identification number N5113K, powered by a 205 horsepower Continental Series E engine. Figure 1 is a picture of the aircraft. This aircraft is an all metal, low wing, single engine airplane with retractable landing gear. There were several modifications made to the basic aircraft necessitating that it be placed in an experimental category during this investigation. The first modification was the installation of a bridge circuit to measure the flap position. This circuit was calibrated to give a cockpit indication of the flap position within  $\pm 0.5$  degrees. A diagram of this circuit is shown in Figure 2.

A second modification was based on the temporary placement (on the ground) of a series of Kiel tubes around the engine housing behind the propeller to measure the dynamic pressure behind the propeller. A survey of this pressure was made and all of the Kiel tubes were removed except one on the top of the cowl at the 0.75 radius station which represented the average dynamic pressure behind the propeller. The output of this total pressure tube was ducted into one side of a conventional airspeed indicator and the other side was connected to the total pressure side of the aircraft's pitot-static tube. When this instrument read zero the dynamic pressure behind the propeller equalled the dynamic pressure as seen by the aircraft out of the propeller's slipstream and indicated zero thrust. Figure 3 shows the instruments mounted on the center rib of the windshield.





The third modification of the aircraft was the installation of a potentiometer to read the elevator angle. Figure 4 shows the schematic of this circuit. This circuit allowed the measurement of the elevator angle to one tenth of a degree. The flap and elevator bridges were calibrated and the curve for the elevator bridge is shown in Figure 5.

The fourth modification consisted of the mounting of an alternate set of wing flaps to which were attached sheet metal vortex generators. These vortex generators were mounted as recommended in Reference 1. There were fourteen vortex generators per wing flap as shown in Figure 6.

The fifth modification was the installation of an angle of attack probe mounted on the right wing of the aircraft. The vane was mounted one chord length ahead of the leading edge and a voltage divider circuit calibrated to read angle of attack of the fuselage reference line was mounted in the cockpit. Figure 7 is the calibration curve for this circuit.

#### WIND TUNNEL

The wind tunnel used in this investigation was the two-dimensional wind tunnel at Princeton University. This tunnel has a test section four feet in height and one foot in span. The lift produced by the model was measured by a series of pressure taps mounted on the top and bottom of the test section. The pressure at each tap was read on a fifty tube manometer bank and the integrated value of this lift manometer



was used to give lift coefficient directly. The drag of the model could be determined by a pressure survey of the model's wake. The individual readings of the drag rake manometer were again integrated to read the model's drag coefficient.

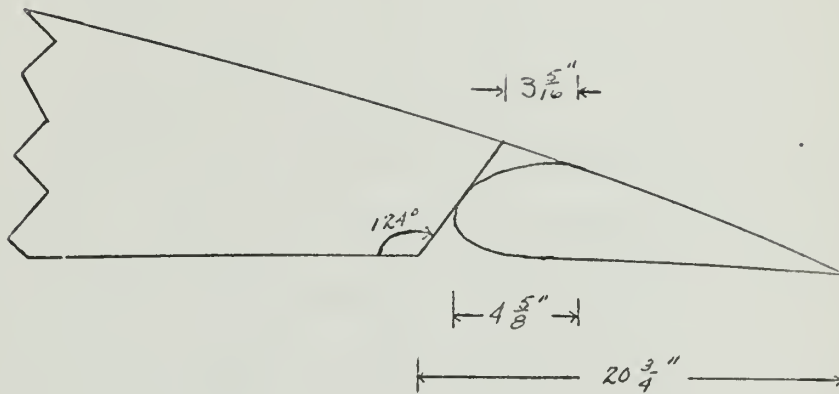
The maximum obtainable tunnel velocity was approximately one hundred fifty miles per hour because of the model size. This includes a tunnel turbulence factor of 1.25.

#### MODEL CONSTRUCTION

In order to determine the feasibility of the idea behind this investigation, a wind tunnel model was constructed. The Navion has a variable wing section, NACA 4415R root section and NACA 6410R tip section. However, in the area of interest, the mid-span of the wing flap, the section was most nearly matched by the NACA 4415R. Thus, the profile of this section was laid out using NACA TR 824 ordinates and a full scale chord of 72 inches. It was decided to absorb the reflex of the wing in the zero deflection setting of the flap of the model, and measurements of the actual wing were made to determine this setting. The flap leading edge, flap port, and hinging geometry were measured and scaled down from the actual aircraft.



This geometry is shown in the sketch below for both the airplane and the model.



#### FLAP SLOT GEOMETRY

The scaling of the model presented a problem because of the limited velocity of the subsonic two-dimensional wind tunnel. The average model size for this tunnel has a span of twelve inches and a chord of about twenty inches. In this case it was decided to use a chord of twenty-five inches in an attempt to attain at least eighty per-cent of full scale Reynold's number. The value of approximately eighty per-cent of full scale Reynold's number was arbitrarily chosen as sufficiently accurate for this experiment.



A two-dimensional model of wood and fiber glass construction was made. The surface of the model was very smooth, and waviness was held to a minimum. Dimensional tolerance was less than  $\pm 0.1$  inches. The flap port was created by bonding a 0.010 inch aluminum strip to the wing portion of the model. The model was mounted in the tunnel using a false tunnel wall to carry the loads into the plastic viewing side of the test section. The entire section was mounted on a twenty-inch diameter disc in order to allow easy variation of angle of attack. Figure 8 shows the model mounted on the false wall.





## PROCEDURES

## INTRODUCTION

When the equipment for this experiment was ready, two areas of investigation were carried out simultaneously. It was necessary to conduct a series of wind tunnel tests on a model to establish the boundary layer thickness, to design the vortex generators, and to see if there was enough of an improvement to proceed with flight testing the modified Navion aircraft. The purpose of the flight testing program was to establish the basic aerodynamic and performance characteristics of the Navion. With these characteristics known, there was a basis of comparison between the modified and unmodified aircraft.

## A) WIND TUNNEL

The first of a series of wind tunnel tests were made to determine the slope of the lift curve of the model and  $C_{l_{max}}$  using the maximum obtainable Reynold's number. First however, since the model had a very smooth surface and since the standard Navion has a stall strip on the leading edge, protruding rivets, lap joints etc., a turbulence trip wire was installed at 10 per cent of the chord of the model. The installation and location of the trip wire was arbitrarily selected to be at the 10 per cent chord station since full scale Reynold's number is of the order of  $6.0 \times 10^6$ , and the transition to turbulent boundary layer must occur fairly early on the actual wing.

The lift curve as a function of angle of attack was recorded at



the maximum obtainable Reynold's number. However, as the angle of attack varied and the flap settings were changed, it was necessary to have a power reserve in order to maintain the tunnel dynamic pressure constant throughout the test. Even so, at full flaps it was not possible to maintain the tunnel's dynamic pressure constant. Further, it was found that a stall was not clearly evident and this was attributed to the size of the model. Since the lift of the tunnel was measured by integrating the pressure differences between the top and the bottom of the tunnel, lift would be recorded by the tunnel even though the airfoil was stalled due to the pressure difference created by the model in the tunnel. The lift curve showed an increase, then a drop, and then a continuing increase in lift as the angle of attack was increased well past any stall angle for a two-dimensional section. The stall angle was obtained by tufting the model and observing the separation of the air flow which corresponded to a drop in the lift curve.

Since it was not possible to run the model at 80 per cent of full scale Reynold's number and vary the flaps, a survey of the boundary layer thickness at zero flap deflection at maximum Reynold's number was made. A value of 98 per cent of free stream velocity was chosen as the boundary layer thickness and a value of 0.45 inches was determined. Then a survey of the boundary layer was made at one-half the obtainable Reynold's number and the boundary layer thickness was found to be 0.50 inches. Since the thickness of the boundary layer was found to be 0.05 inches greater at one-half the full scale Reynold's number, it was decided to run the



tests at the reduced value of the Reynold's number and extrapolate the boundary layer thickness to full scale Reynold's number. This procedure insured an adequate power reserve in the tunnel and constant dynamic pressure for the remaining tests. The lift curve was recorded as a function of angle of attack for the three flap settings of zero, one-half, and full flaps, corresponding to 0, 22, and 44 degrees respectively.

An estimation of the boundary layer thickness at zero flap deflection was made assuming an all turbulent boundary layer. The von Kármán flat-plate formula, given below, was used.

$$\delta = \frac{0.376 X}{\left(\frac{VX}{\nu}\right)^{1/5}} \quad (1)$$

where

$\delta$  = boundary layer thickness, inches

$X$  = chordwise station, feet

$V$  = free stream velocity, feet/second

$\nu$  = kinematic viscosity, square feet/second

In applying the flat plate formula to the airfoil model, the actual tunnel speed was increased by 20 per cent to allow for airfoil curvature, and the kinematic viscosity was computed for a tunnel temperature of 90<sup>0</sup> F. On the basis of these assumptions, the boundary layer thickness at the 80 per cent chord station was computed to be 0.39 inches.

After the model lift curves were determined, it was necessary to design the vortex generators. Using the design criteria given in Reference 1,



small vortex generators were manufactured out of 0.010 inch aluminum and mounted on the flap of the model at various angles of attack. The angles of attack selected were 5, 10, and 15 degrees. Reference 1 recommended a vortex generator span of 1.2 times the local boundary layer thickness, and a tip chord of 1.6 times the span. In addition, two sizes of vortex generators were used. The span of the second set was 0.6 times the local boundary layer thickness and the tip chord was 0.8 times the span. The wind tunnel results indicated that vortex generators with a span of 1.2 times the local boundary layer thickness set at 5 degree angle of attack were optimum.

#### FLIGHT TESTING

The flight test crew consisted of a pilot and copilot observer. The copilot acted as a safety observer since Princeton University is located in a rather high density air traffic area. The copilot also recorded the data and operated the test equipment.

The first area of investigation was the lift and drag of the airplane. The values of lift and drag were determined by gliding the aircraft. After a climb to altitude, a constant speed glide was established, and the throttle adjusted so that the dynamic pressure behind the propeller equalled the dynamic pressure as measured by the aircraft's pitot-static system. This procedure eliminated the thrust vector from the force polygon of the aircraft. After the glide was established, the rate of sink in feet per minute was measured by using a stop watch and the altimeter. With the rate of sink, the flight velocity, and the aircraft weight known, determination of the glide angle enabled computation





of the lift and drag. Weight was determined by weighing the aircraft, and was found to be 2203 pounds including full fuel and oil. The largest source of error in weight determination was the inflight measurement of total fuel on board due to gauge inaccuracy. Thus, the fuel on board was measured by flight time and known engine fuel consumption was checked after the flight by topping off the tanks on the ground. This procedure was accurate to  $\pm 2$  gallons, or 12 lbs. of weight, which was sufficiently accurate for this investigation.

By measuring atmospheric pressure and outside air temperature, the density was calculated by using

(2)

$$\rho = \frac{P}{gRT}$$

With the density

known, the non-dimensional coefficients,  $C_D$  and  $C_L$ , were next determined.

Since

(3)

$$C_D = C_{Df} + \frac{C_L^2}{\pi A e},$$

plotting  $C_D$  versus  $C_L^2$ , resulted in a linear relationship. By cross plotting  $C_D$  versus  $C_L^2$  and  $C_D$  versus  $C_L$ , accurate airplane polar curves could be drawn. Further, these polar curves gave the value of minimum drag,  $C_{D0}$ , and the slope gave the Oswald efficiency factor,  $e$ .

The slope of the lift curve was measured by using the angle of attack vane. The aircraft was flown at constant altitude and airspeed, and by knowing the weight and recording the angle of attack,  $C_L$  versus



the angle of attack of the fuselage reference line could be calculated. The slope of the lift curve,  $C_{L\alpha}$ , was determined for zero, one-half, and full flaps.

The value of  $C_{L_{max}}$  versus flap deflection was obtained in a similar manner. In this case it was necessary to define the stall point of the Navion. As the stall was approached and the power was reduced, an airspeed was reached at which the aircraft could not be flown at constant altitude. This occurred at 2 to 3 MPH before a definite stall occurred as indicated by a sharp drop in the nose attitude. This value was selected as the stall speed and the calculations for  $C_{L_{max}}$  are based upon this airspeed.

The elevator angle to trim, which is an indication of the downwash, was measured by the bridge circuit described in the Equipment section. Constant airspeed and altitude were held while the aircraft was trimmed for zero pitching moment, and the elevator angle was measured.

#### POWER REQUIRED

As an indication of the drag of the aircraft, power required versus velocity in level flight was determined. Prior to take-off the fuel was topped off and the tests were conducted immediately after takeoff and climb to altitude. This had the effect of removing gross weight as a variable since the fuel consumption rate was not of sufficient magnitude to affect the final reduced data.

The tests were flown at constant pressure altitude ( $h_p$ ) where outside air temperature (deg. C.), manifold pressure (in.  $H_g$ ), engine RPM and airspeed (MPH) were recorded. Data thus obtained was converted to sea level, standard day conditions by conventional techniques. The



brake horsepower for each power setting was then obtained graphically from Continental Series E. engine performance curves.

Tests were conducted at flap deflections of zero, one-half, and full, and a comparison was made between the aircraft with and without the vortex generators.



## RESULTS

## A) WIND TUNNEL TEST RESULTS

The results of the tests conducted in the Princeton University two-dimensional, subsonic wind tunnel are presented in Figures 9 through 13. Figures 9 and 10 establish the validity of conducting the wind tunnel tests at one-half full scale. Reynold's number as they show the small variation with Reynold's number of the lift coefficient versus angle of attack, for the model with no vortex generators attached. Figure 11 shows the effect of angle of attack of the vortex generator,  $\alpha_g$ , on  $c_l$  versus  $\alpha$  when the height of the vortex generator was 1.2 times the boundary layer thickness. Figure 12 shows the same information for vortex generators with a height of 0.6 times the boundary layer thickness. Comparison of these curves indicated that the maximum increment in lift coefficient  $\Delta c_l$ , was obtained when the large vortex generators were attached to the flap with  $\alpha_g = 5$  degrees and with full flap deflection. This increment is shown in figure 13.

The values of section lift coefficient were obtained by converting the change in the height of fluid in the integrating lift manometer according to the following formula:

$$c_l = \frac{K_l \ell}{q c} \quad (4)$$

where  $q$  = dynamic pressure - lb/ft<sup>2</sup>  
 $c$  = model chord ft.





$l$  = manometer height change - inches

$$K_L = 4.79 \frac{\Delta H}{\Delta L} \text{ -- lb. lift/inch travel}$$

$\Delta H$  is an arbitrary change in the height of the fluid in six of the fifty tubes of the manometer bank while  $\Delta L$  is the height change of the fluid in the integrating manometer resulting from  $\Delta H$ . Calibration of the manometer and determination of  $K_L$  was made prior to each series of tests.

Reynold's number was computed based on the chord of the section.

## B) FLIGHT TEST RESULTS

The results of the flight test portion of this investigation are shown in Figures 14 through 26. Values of maximum lift coefficient over the range of flap deflections with power off are shown in Figure 14. Figure 15 shows the values of maximum lift coefficient as a function of power required to maintain level flight for the various flap settings. This data has been reduced to sea level, standard day conditions.

Figures 16 through 18 show the parabolic polar approximations which are based on the formula

$$C_D = C_{D_f} + \frac{C_L^2}{\pi A e} \quad (5)$$

By cross-plotting this linear relationship and the actual lift and drag coefficients, the airplane polar curves, Figures 19 through 21, were constructed.

The values of elevator deflection angle required to trim in level flight as a function of airspeed for the three flap deflections are



shown in Figures 22 through 24.

The basic performance curve (power required versus velocity) is presented for sea level, standard day conditions in Figure 25. This data is shown for the airplane with and without vortex generators installed, and for the three primary flap deflections. Figure 26 is a plot of lift coefficient versus angle of attack of the fuselage reference line for the three flap conditions.



## DISCUSSION

The problem presented for solution is best stated by referring to Figure 27 which shows the basic Navion flap which has been tufted. Figure 27A illustrates that in the cruise configuration the flow is attached over the entire flap. Figure 27B indicates that in the one-half flap position some flow separation occurs at the trailing edge of the flap while in Figure 27C the flow is seen to be reversed from 50 per cent of the chord of the flap to the trailing edge, and to be separated forward of the 50 per cent flap chord station when in the approach configuration with full flap deflection.

This same phenomenon was observed on the wind tunnel model prior to the installation of the vortex generators. The first encouraging information was obtained when it was noted that flow separation at full flap deflection was delayed with the application of the vortex generators. This was especially noticeable in the flow downstream of the pairs of vortex generators forming convergent nozzles. This delay of flow separation was also evident in flight, although to a lesser degree.

With a partial reattachment of the flow, it was assumed that an increase in maximum lift coefficient would be obtained with the application of the vortex generators. The wind tunnel tests verified this assumption and indicated that the largest increase in maximum lift coefficient would be obtained by attaching vortex generators with a span of 1.2 times the local boundary layer thickness at an angle of five degrees to the free stream flow. At this point it must be noted that the vortex



generators used on the wind tunnel model were flat plates.

With the knowledge that the vortex generators did in fact produce beneficial results when applied to a wind tunnel model, their application to the flaps of the Navion was undertaken. A second set of flaps was obtained for this purpose. Since Reference 1 reported favorable results in a similar situation using a NACA 64<sub>1</sub>-812,  $a = 0.3$  airfoil as a vortex generator, the decision was made to use thin plates cambered to conform to this mean line as the vortex generators for the Navion. These vortex generators were manufactured with a span of 2.32 inches (1.2 times the local boundary layer thickness) and a root chord of 4.95 inches. A taper ratio of 0.75 was used resulting in a tip chord of 3.72 inches. These dimensions resulted from using the design criteria given in Reference 1. These vortex generators were then attached to the flap as shown in Figure 6, with the chord line set at an angle of attack of five degrees to the free stream flow. The vortex generators were spaced seven inches apart, measured from the leading edge.

A comparison of the results of the flight tests conducted with the basic versus the modified Navion revealed a decrease in the maximum lift coefficient for the modified aircraft (Figure 14). Further investigation of the wind tunnel results (Figures 10, 11, and 13) led to the conclusion that because of the camber of the vortex generators mounted on the aircraft, the vanes were operating very nearly like flat plate vortex generators mounted at an angle of ten degrees. The possibility of this effect is indicated in Figure 28 which compares the angle of attack required to generate a given lift





coefficient by a two-dimensional flat plate and the two-dimensional NACA  $a = 0.3$  mean line.

Since the wind tunnel results had shown that although the increase in maximum lift coefficient for vortex generators set at ten degrees angle of attack was significant, it was not as large an increase as would be realized had the vortex generators been set at a five-degree angle of attack. Because of the location of the vortex generators on the wing at a flat plate angle of attack of ten degrees, the decrease in maximum lift coefficient in the zero and half flap condition for both power-on and power-off level flight was attributed to the vortex generators acting as spoilers. The vortex generators acting as spoilers would reduce the maximum lift coefficient in both cases.

As was expected, the primary advantage of the vortex generators was realized in the approach configuration with full flap deflection. Here the effect of power was to add sufficient momentum to the boundary layer so that the increased effective angle of attack of the vortex generators was no longer detrimental. In level flight an increase in maximum lift coefficient for a given brake horsepower was obtained (Figure 15), and the "back side" of the power curve was eliminated (Figure 25). This would indicate that for a power-on approach the speed could be reduced approximately ten miles per hour from the approach speed recommended by the manufacturer resulting in a shorter landing roll.



A decrease in the total drag coefficient was also realized in this configuration (Figure 21). Although Figure 18 indicates an increase in profile drag, the Oswald efficiency factor is increased, thereby causing a reduction in the induced drag. This reduction predominates. A further decrease in drag was a result of the reduction in pressure drag caused by the delay in flow separation resulting from the application of the vortex generators.

At the flap settings of zero and one-half deflection, the presence of the vortex generators, as installed, was definitely undesirable. This was a result, primarily, of the rather significant increase in profile drag (Figures 16 and 17). Figure 25 shows this same effect as an increase in power required for level flight. For example, in the cruise configuration at 130 miles per hour and assuming 30 gallons of fuel available for cruise, a reduction in range of 84 miles, or 18.3 per cent, would be caused by the vortex generators. This reduction in range would be unacceptable in most instances, and therefore establishes the requirement for further investigation to determine the optimum size, shape and location of the vortex generators. This further investigation hopefully would also lead toward the elimination of reversal of the decrease in maximum lift coefficient evidenced in Figure 15. The vortex generators had no effect on the lift curve slope (Figure 26).

The presence of the vortex generators on the flaps introduced no apparent change in the handling qualities of the airplane. Figures 22 through 24 show that the elevator deflection required to trim the aircraft at speeds throughout the tested range was not significantly increased, and in the cases of one-half and full flap deflection was



decreased. Sufficient elevator power was available at all times and the airplane exhibited static and dynamic stability in all modes save the spiral mode. This spiral instability was not aggravated by the presence of the vortex generators.



## CONCLUSIONS

The proposed employment of vortex generators is a feasible idea but further investigation must be conducted before they can be gainfully employed.

From the wind tunnel tests, it can be concluded that vortex generators will give a significant lift coefficient increase.

From the flight test program it can be concluded:

1. That a significant drag increase can be expected for zero and half flap settings. This would indicate that the vortex generators should be connected to the flap actuators and retracted when the flaps are raised.
2. That the application of vortex generators in the full flap condition eliminated the back side of the power curve.
3. That the vortex generators, in the full flap setting, give a significant reduction in drag coefficient which should give a reduction in take-off roll.
4. That the vortex generators in this investigation acted as spoilers and gave approximately a 5 per cent reduction in maximum lift coefficient for power-on and power-off conditions, except for the full flap case in which there was a 5 degree increase in maximum lift coefficient.
5. That for further investigation care should be taken not to "over generate". Perhaps a vortex generator in the form of a T with the top an airfoil of a delta planform





would prove more advantageous.

6. That there was no significant aerodynamic or stability change in the aircraft.



## REFERENCE AND BIBLIOGRAPHY

United Aircraft Corporation Research Department Report No. R-05280-9, "United Aircraft Research Department Summary Report on Vortex Generators," by Taylor, H. D. 1950.

Airplane Performance, Stability and Control, by Perkins, Courtland D. and Hage, Robert E. 1949. John Wiley and Sons, Inc. New York.

NACA Report No. 824, "Summary of Airfoil Data," by Abbott, I. A., von Doenhoff, A. E. and Stivers, L. S., Jr. 1945.

Unpublished notes of Professor H. G. Koehler, Department of Aeronautics, U. S. Naval Postgraduate School. Monterey, California. 1959.

Engineering Applications of Fluid Mechanics, by Hunsaker, J. C. and Rightmire, B. G. 1947. McGraw-Hill Book Company, Inc. New York.



## LIST OF FIGURES

1. Port Aircraft
2. Flap Deflection Circuit
3. Flap Deflection Instrument Panel
4. Elevator Deflection Circuit
5. Elevator Calibration Curve
6. Modified Flaps
7. Angle of Attack Calibration Curve
8. Wind Tunnel Model
9.  $C_L$  vs.  $\alpha$  2.5  $N_R$  clean
10.  $C_L$  vs.  $\alpha$  1.25  $N_R$  clean
11.  $C_L$  vs.  $\alpha$  1.25  $N_R$  Large Vortex Generators
12.  $C_L$  vs.  $\alpha$  1.25  $N_R$  Small Vortex Generators
13.  $\Delta C_L$  increase vs. vortex generator size and  $\alpha_g$
14.  $C_{Lmax}$  vs.  $\delta_f$
15. Power Required vs.  $C_{Lmax}$
16.  $C_D$  vs.  $C_L^2$   $\delta_f = 0$
17.  $C_D$  vs.  $C_L^2$   $\delta_f = 22^\circ$
18.  $C_D$  vs.  $C_L^2$   $\delta_f = 39^\circ$
19.  $C_D$  vs.  $C_L$   $\delta_f = 0^\circ$
20.  $C_D$  vs.  $C_L$   $\delta_f = 22^\circ$
21.  $C_D$  vs.  $C_L$   $\delta_f = 39^\circ$
22.  $\delta_e$  vs. Velocity  $\delta_f = 0^\circ$
23.  $\delta_e$  vs. Velocity  $\delta_f = 22^\circ$
24.  $\delta_e$  vs. Velocity  $\delta_f = 39^\circ$



- 25. Power Required vs. Velocity
- 26.  $C_L$  vs.  $\alpha$  FRL
- 27. Photographs of Flow Separation
- 28. Effects of Camber on  $C_L$  vs.  $\alpha$







**RYAN NAVION**

**FIGURE 1**



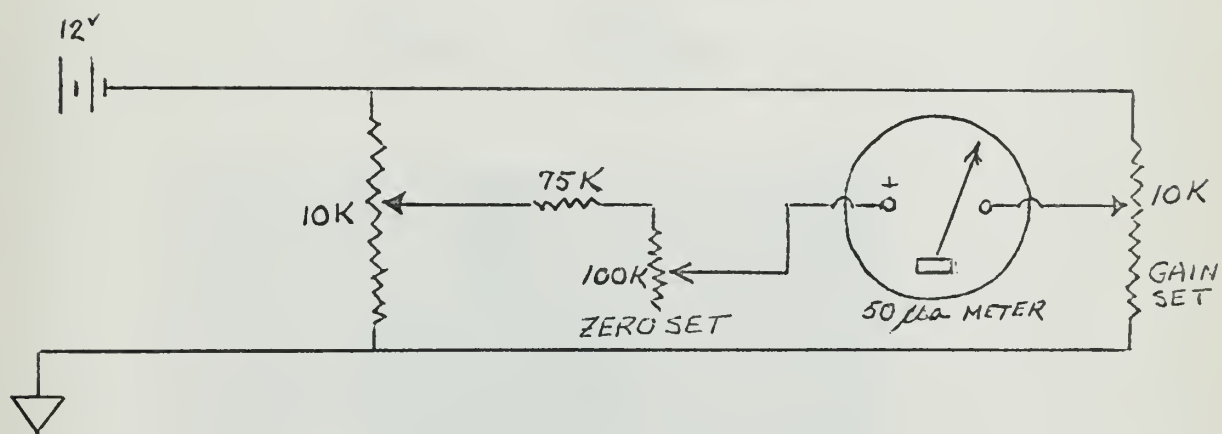
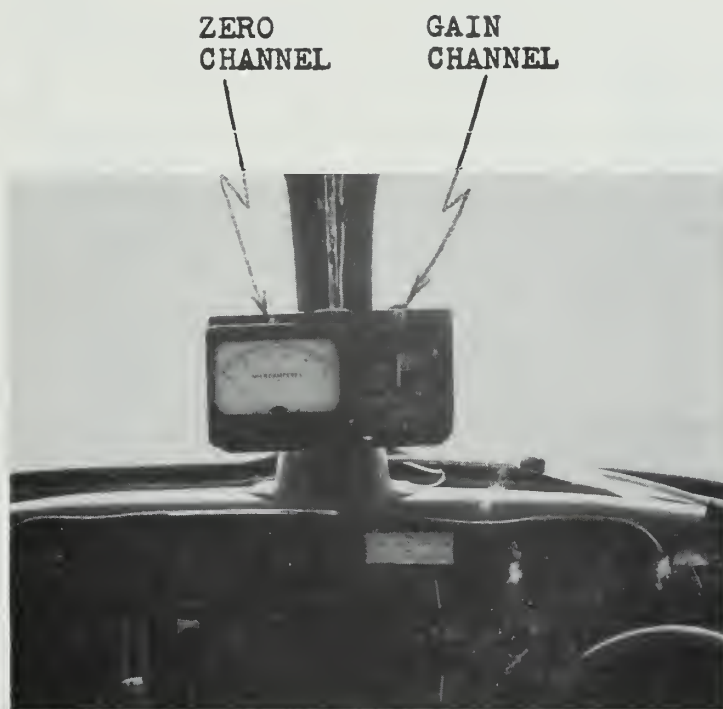


Fig- 2

FLAP INDICATOR CIRCUIT DIAGRAM





FLAP DEFLECTION METER AND THRUSTMETER CONSOLE

FIGURE 30



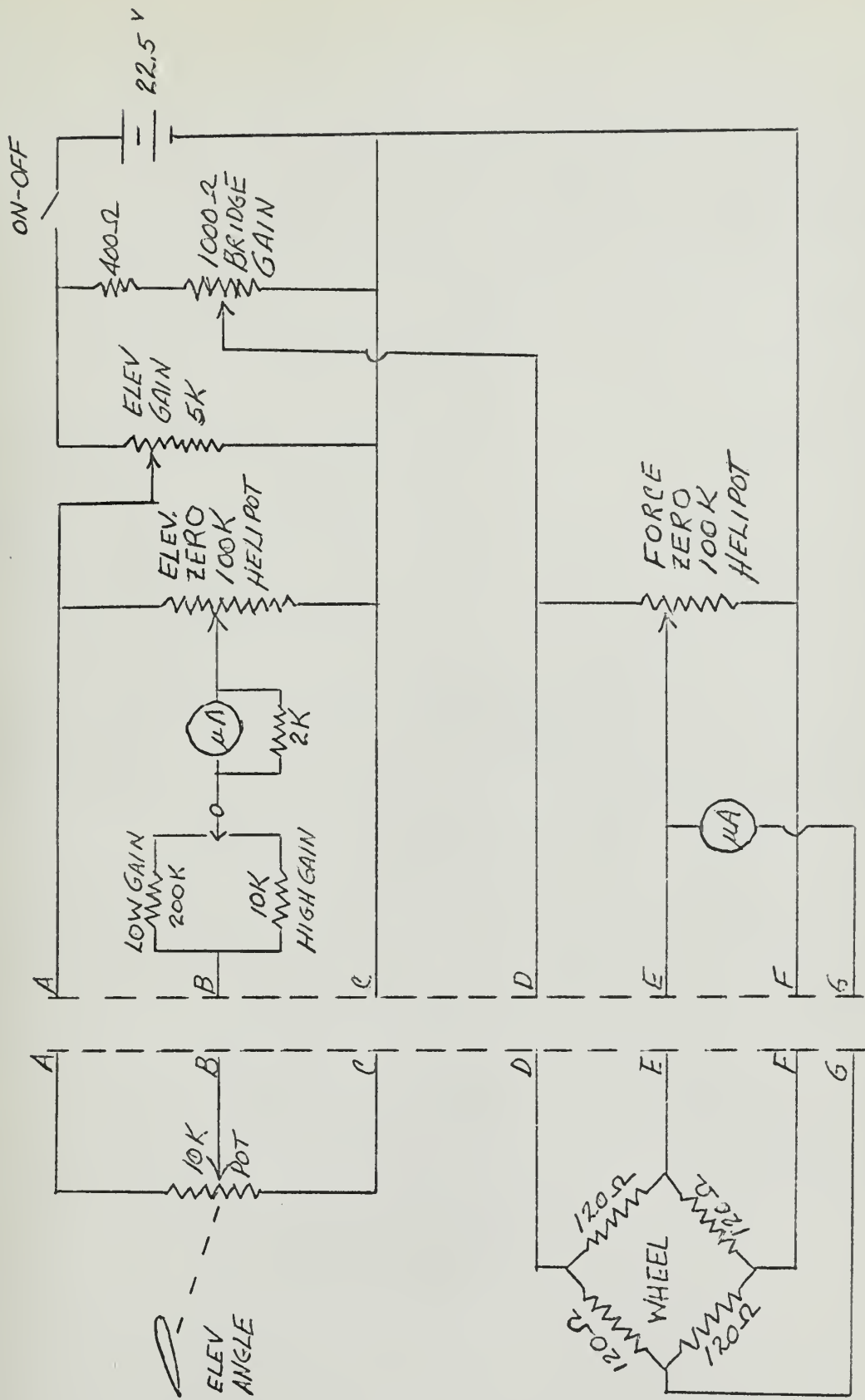
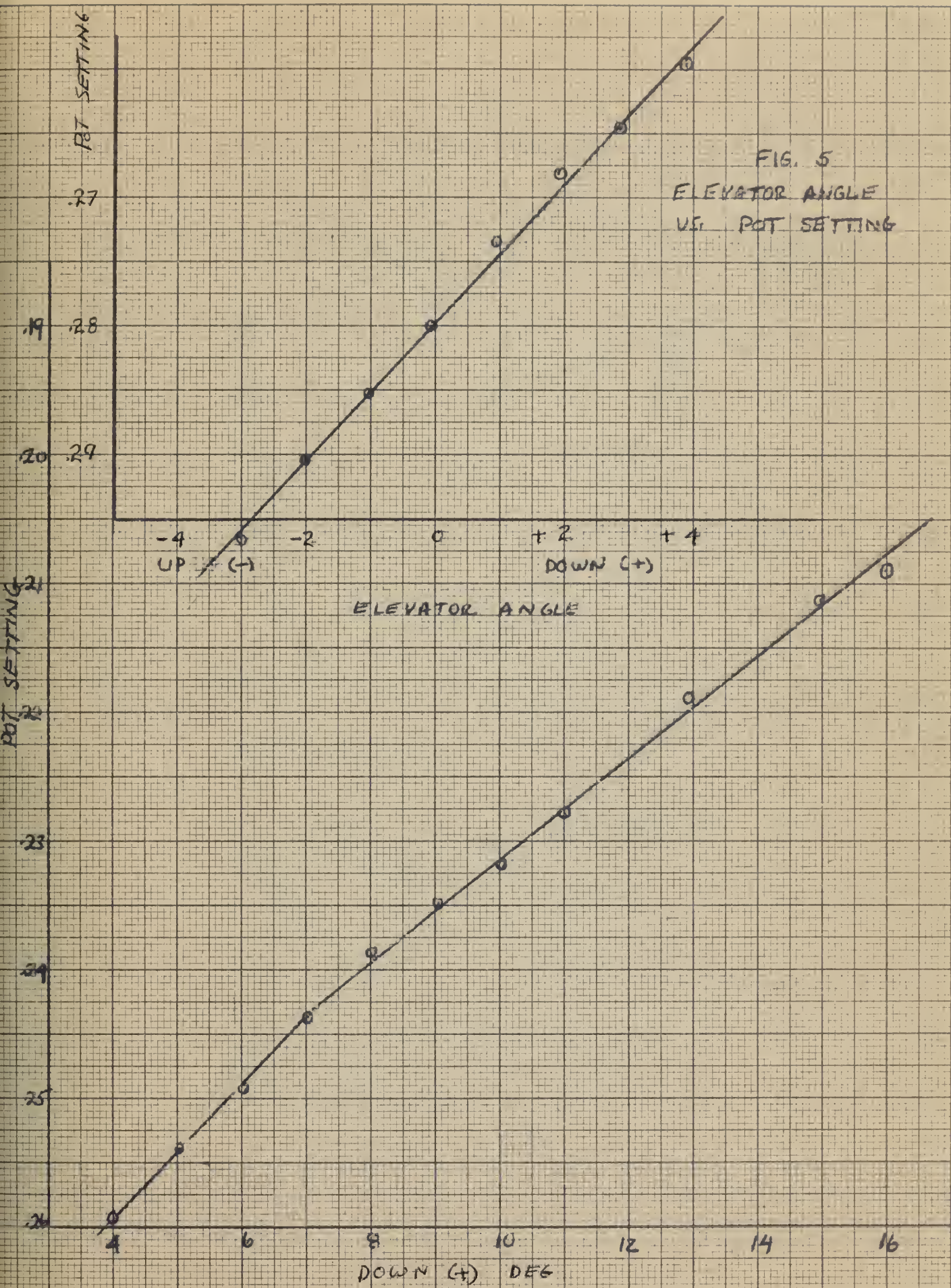


Fig. 4  
INSTRUMENTATION CIRCUIT DIAGRAM







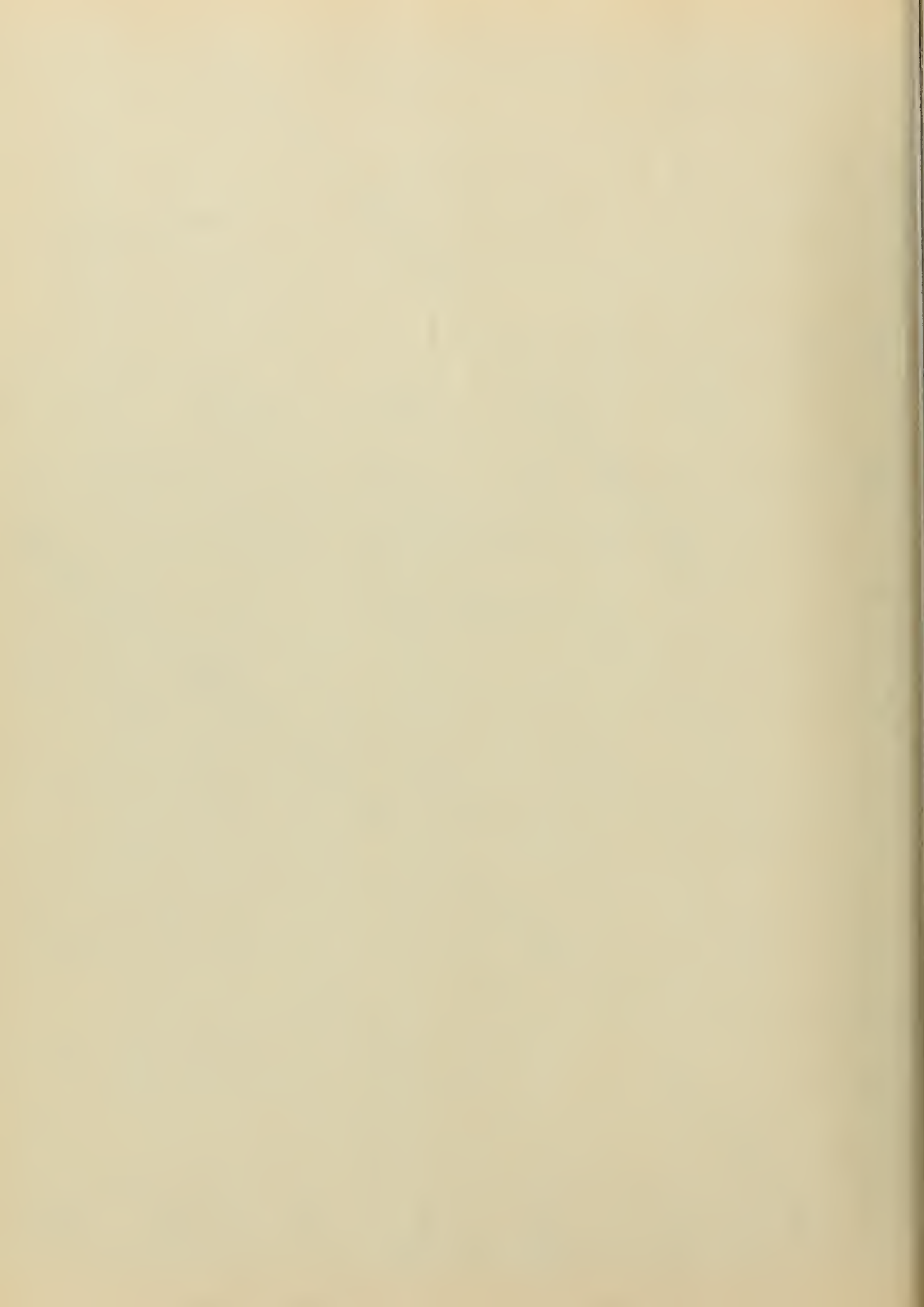


FIGURE 6  
MODIFIED FLAPS

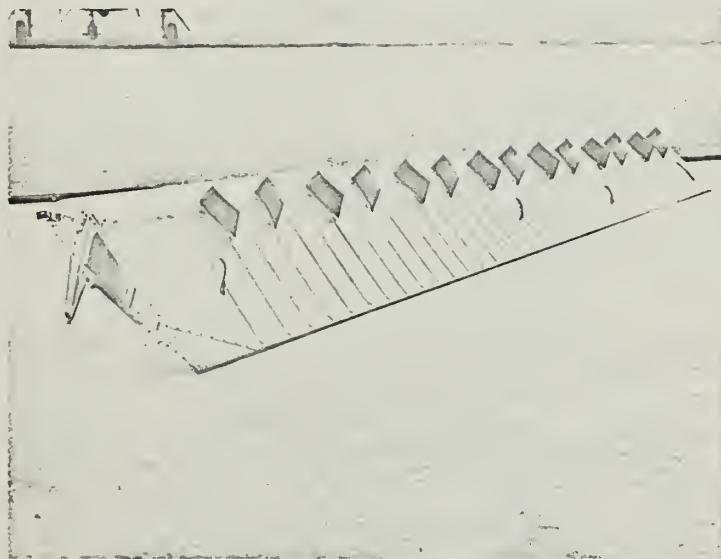
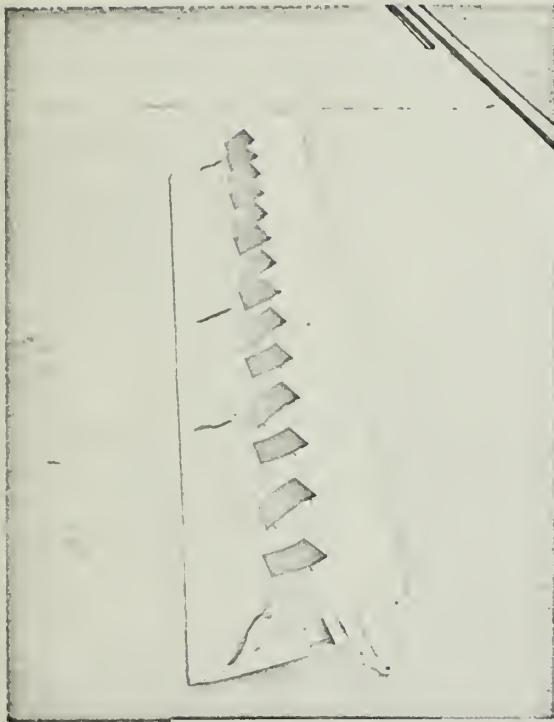






FIG. 7  
ANGLE OF ATTACK  
INSTRUMENTATION CALIBRATION

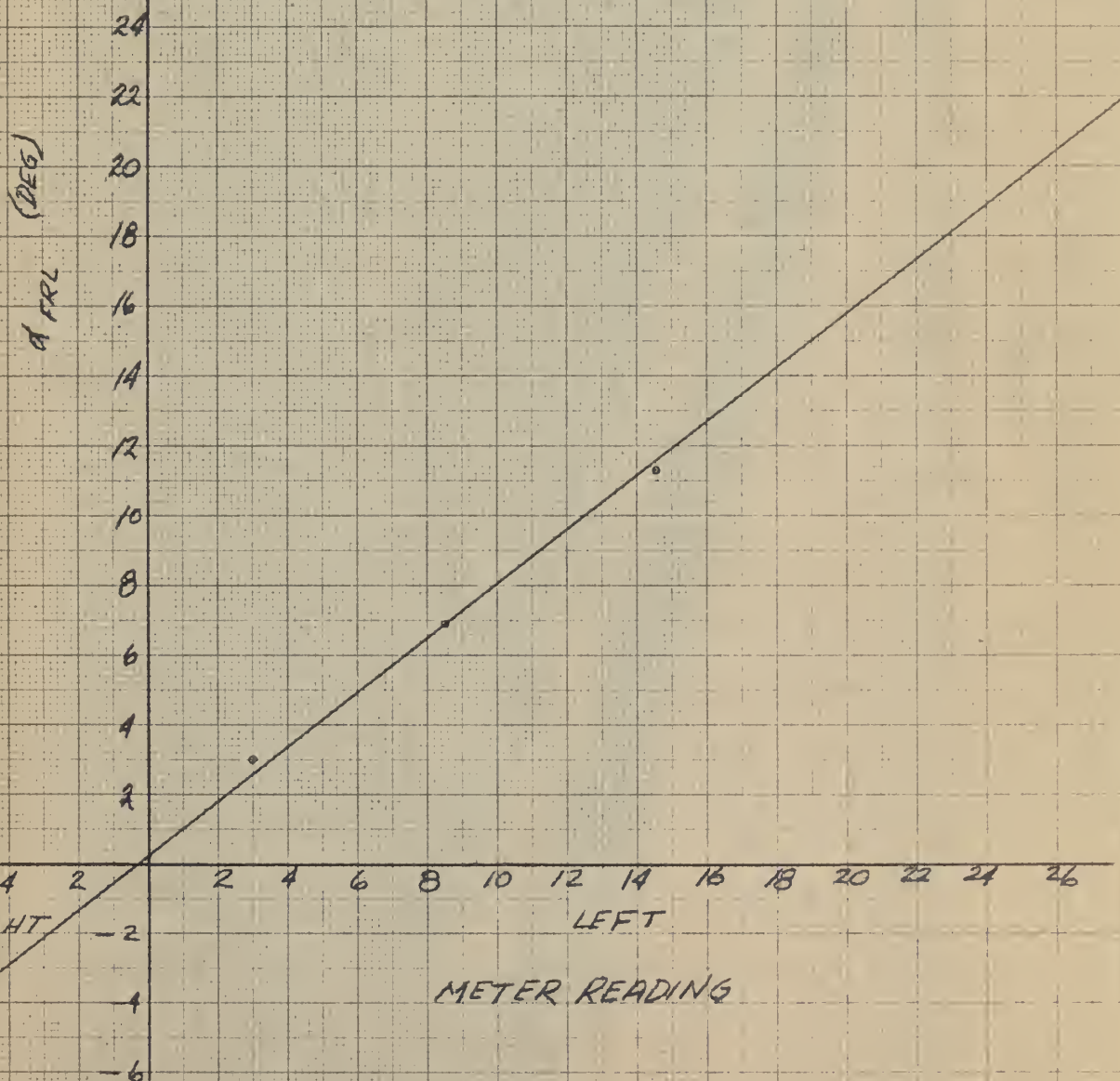






FIGURE 8  
WIND TUNNEL MODEL





FIG. 9  
SECTION LIFT COEFFICIENT  
VS.  
ANGLE OF ATTACK  
 $N_R = 2.5 \times 10^6$   
NO VORTEX GENERATORS

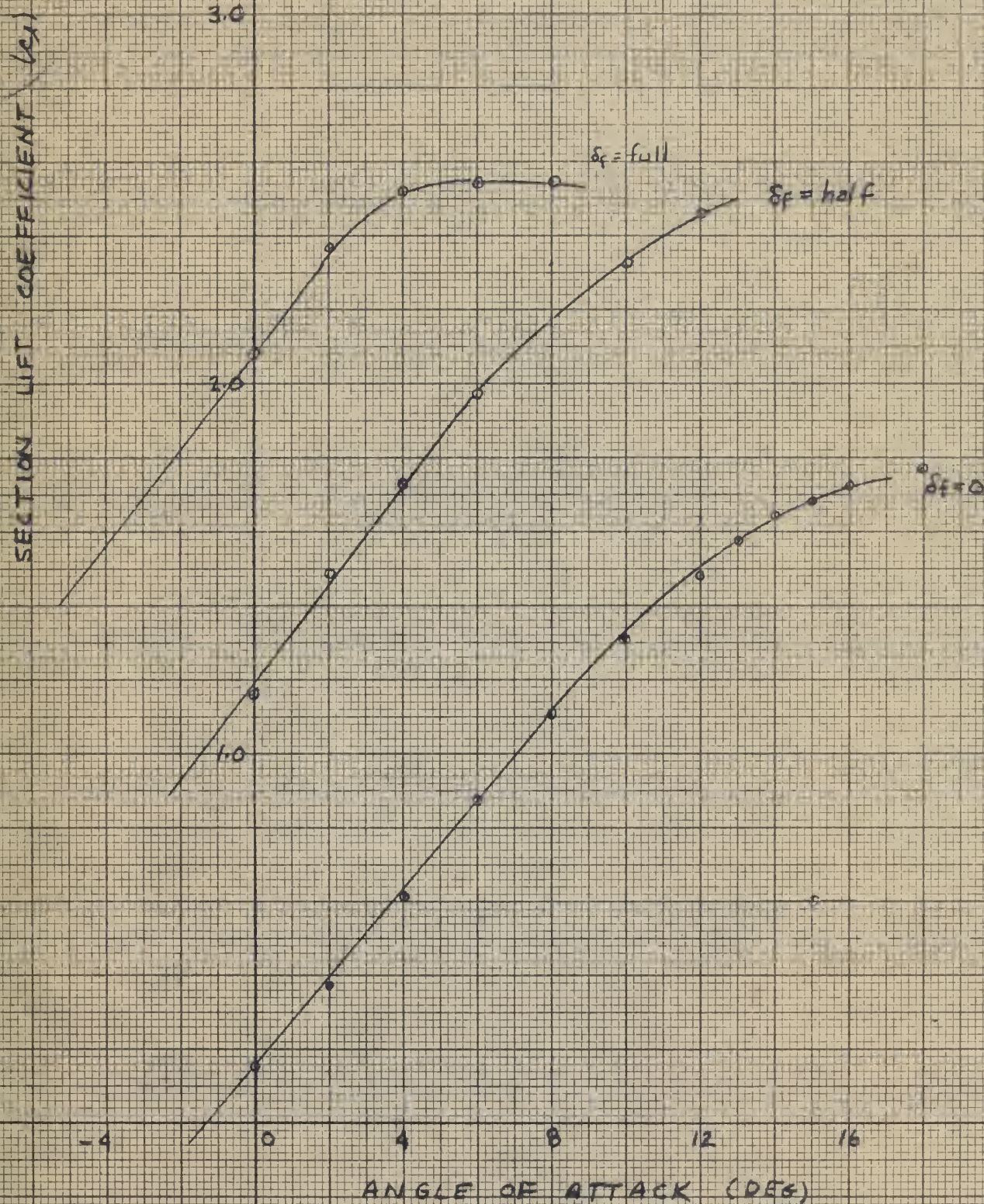
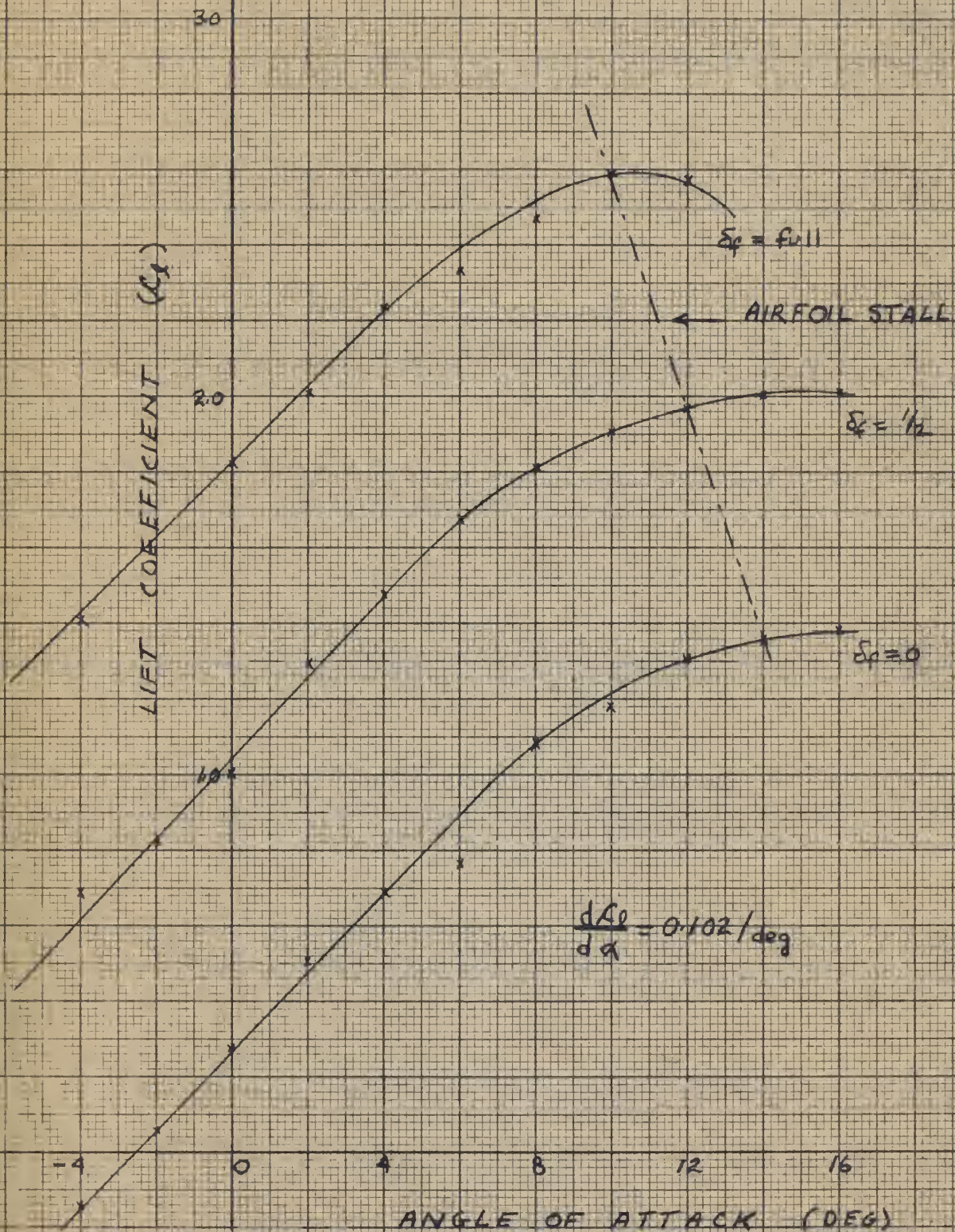






FIG. 10

SECTION LIFT COEFFICIENT  
VERSUS ANGLE OF ATTACK  
NO VORTEX GENERATORS  
TRIP WIRE;  $N_R = 1.25 \times 10^6$



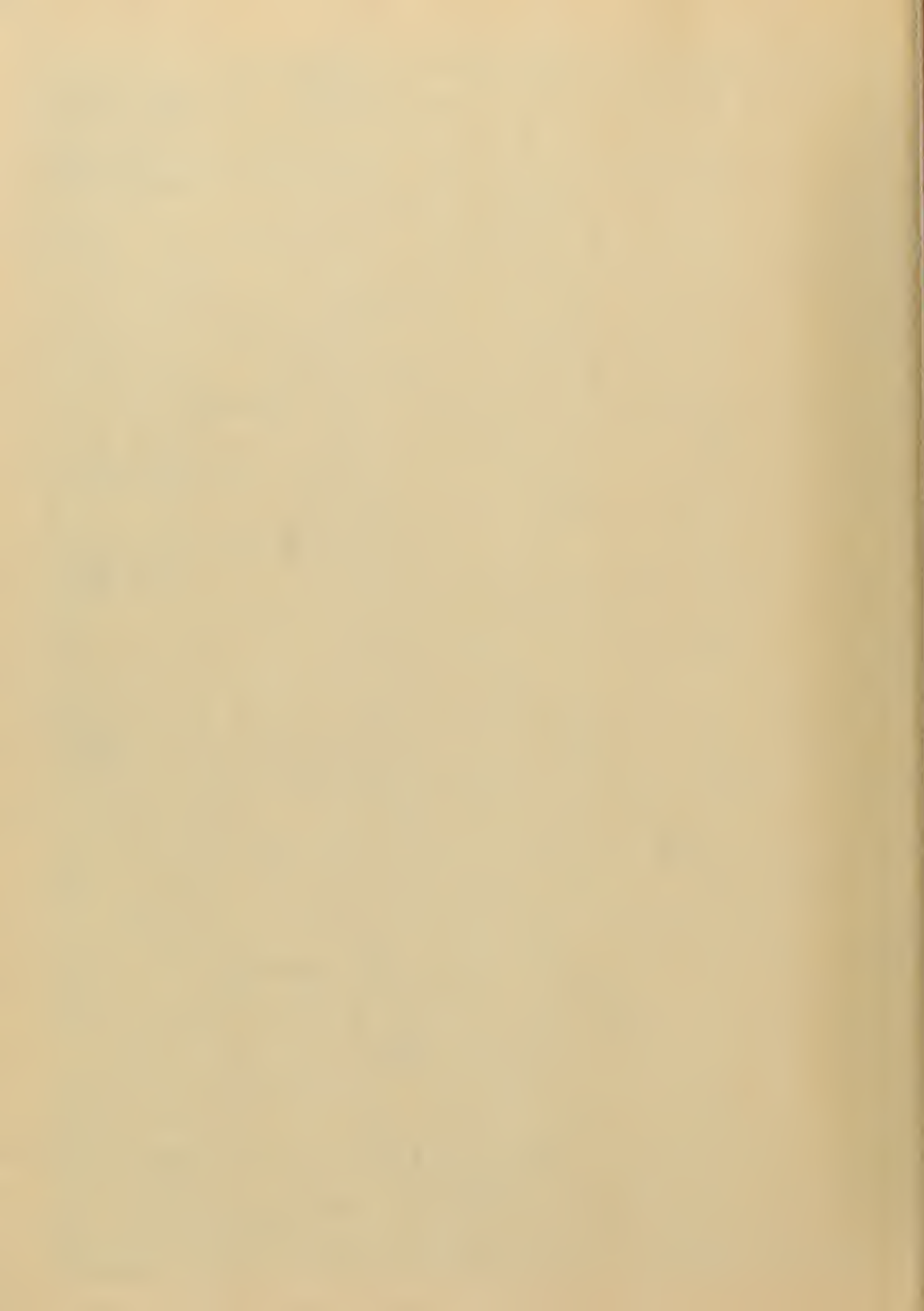
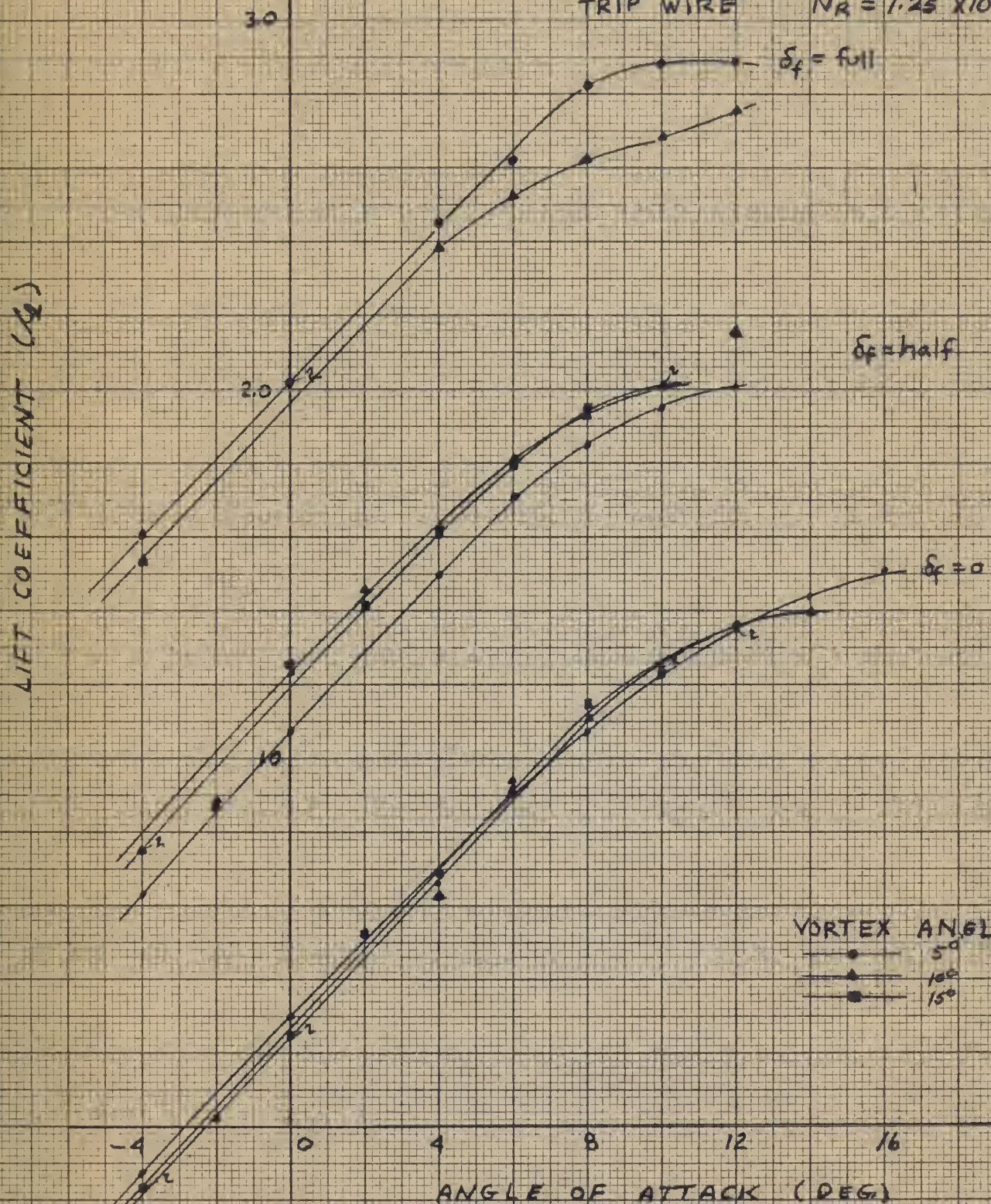




FIG. 11  
SECTION LIFT COEFFICIENT  
VS.  
ANGLE OF ATTACK  
VORTEX GENERATORS 1.2"X12"  
TRIP WIRE  $N_R = 1.25 \times 10^6$



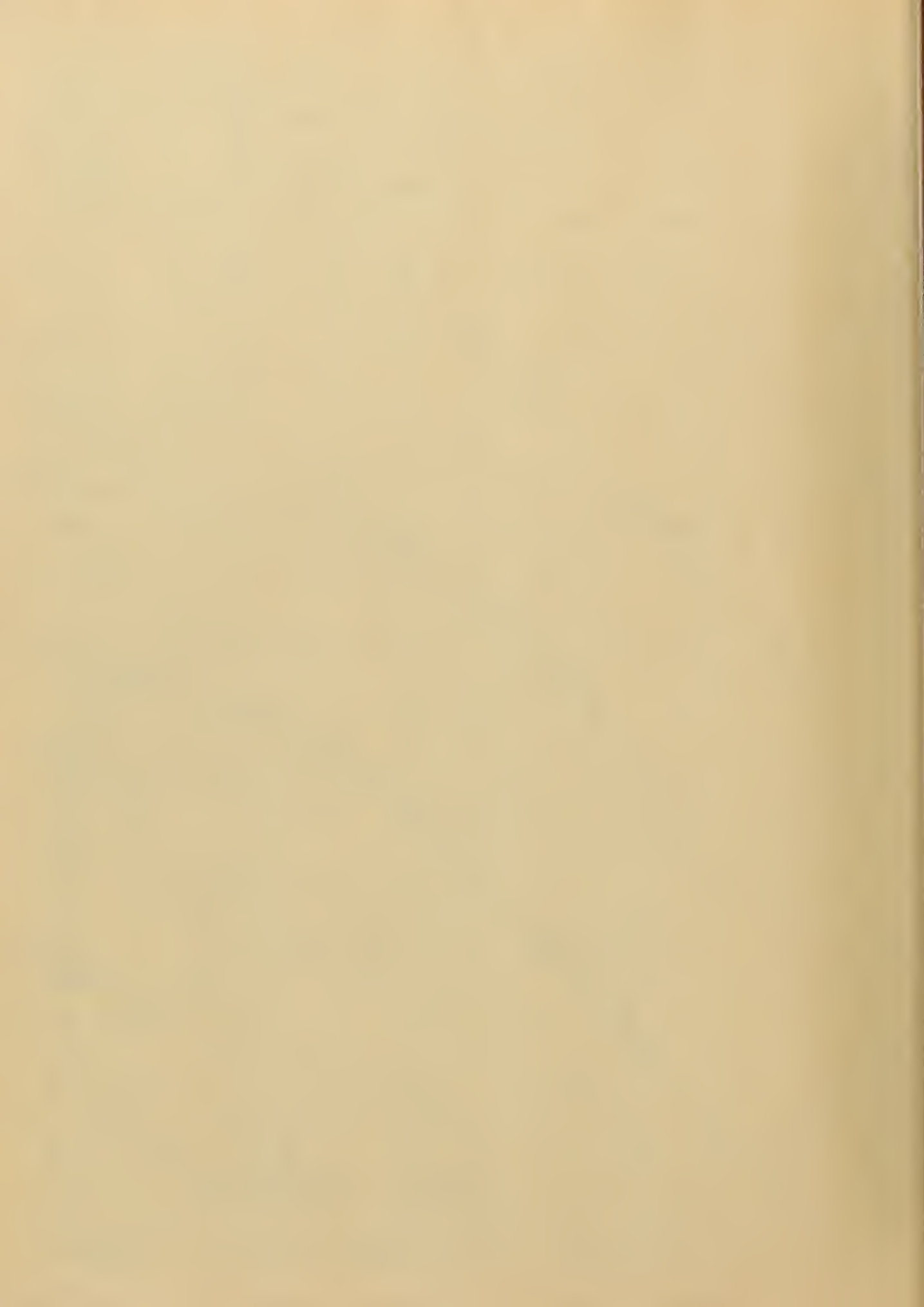
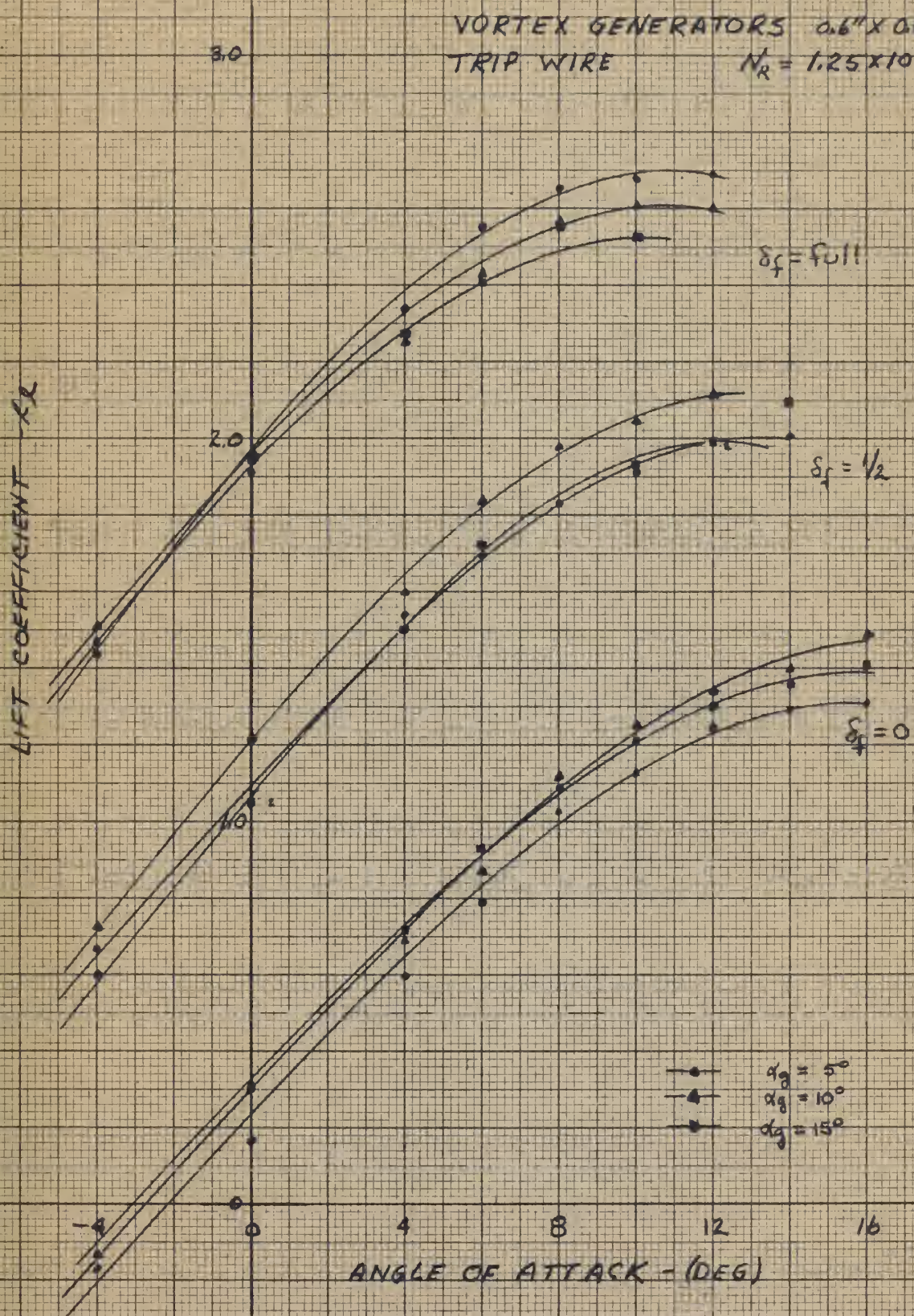
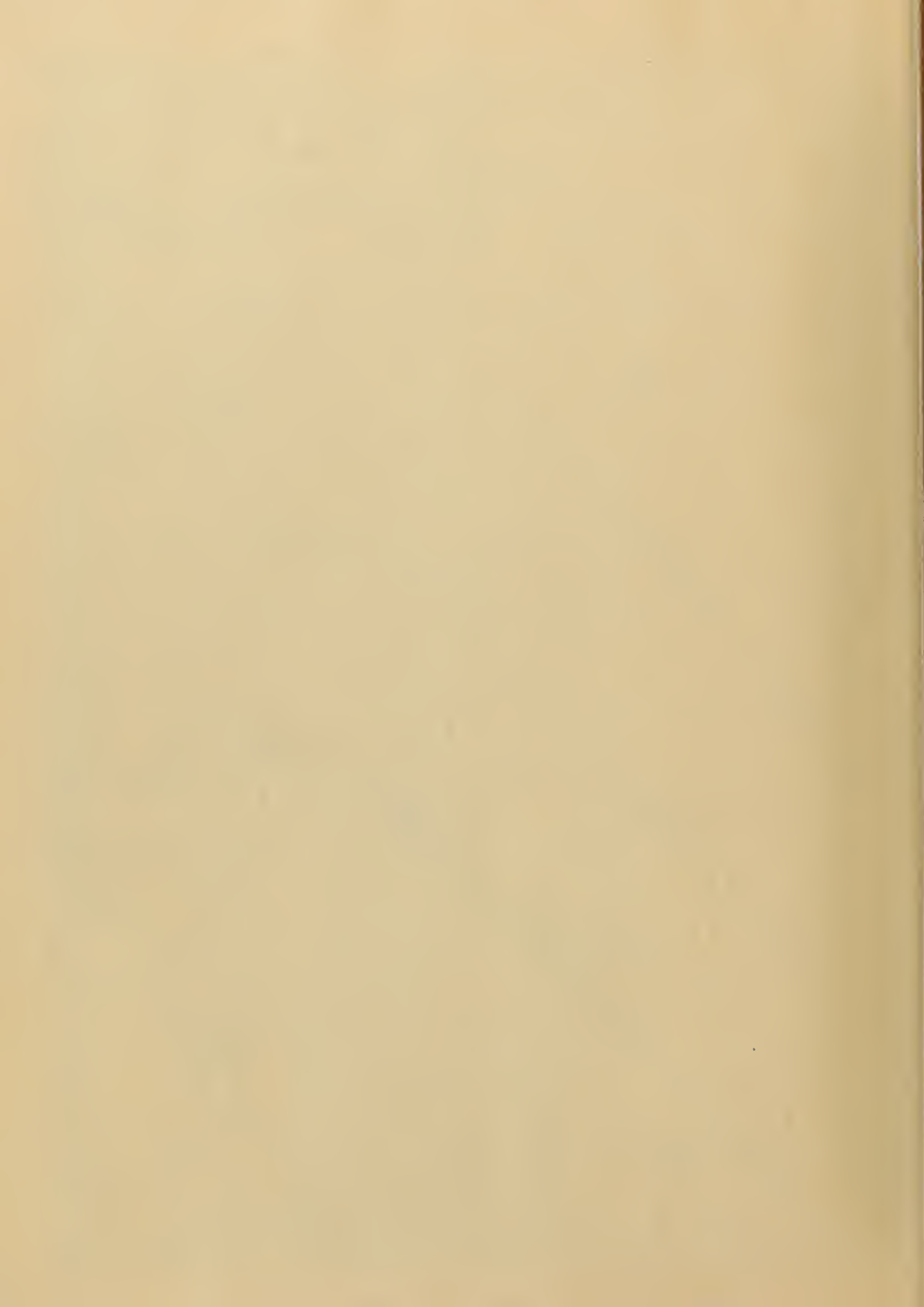




FIG. 12  
SECTION LIFT COEFFICIENT  
VS  
ANGLE OF ATTACK

VORTEX GENERATORS 0.6" X 0.6"  
TRIP WIRE  $N_R = 1.25 \times 10^6$







LIFT COEFFICIENT INCREMENT  $\Delta C_L$

FIG. 13  
EFFECT OF VORTEX  
GENERATOR SIZE & ANGLE ON  
SECTION LIFT COEFFICIENT  
 $\delta_{+} = \text{FULL}$

- $\alpha_g = 5^\circ$  } LARGE V.G.
- $\alpha_g = 10^\circ$  }
- $\alpha_g = 5^\circ$  } SMALL V.G.
- $\alpha_g = 10^\circ$  }
- $\alpha_g = 15^\circ$  }

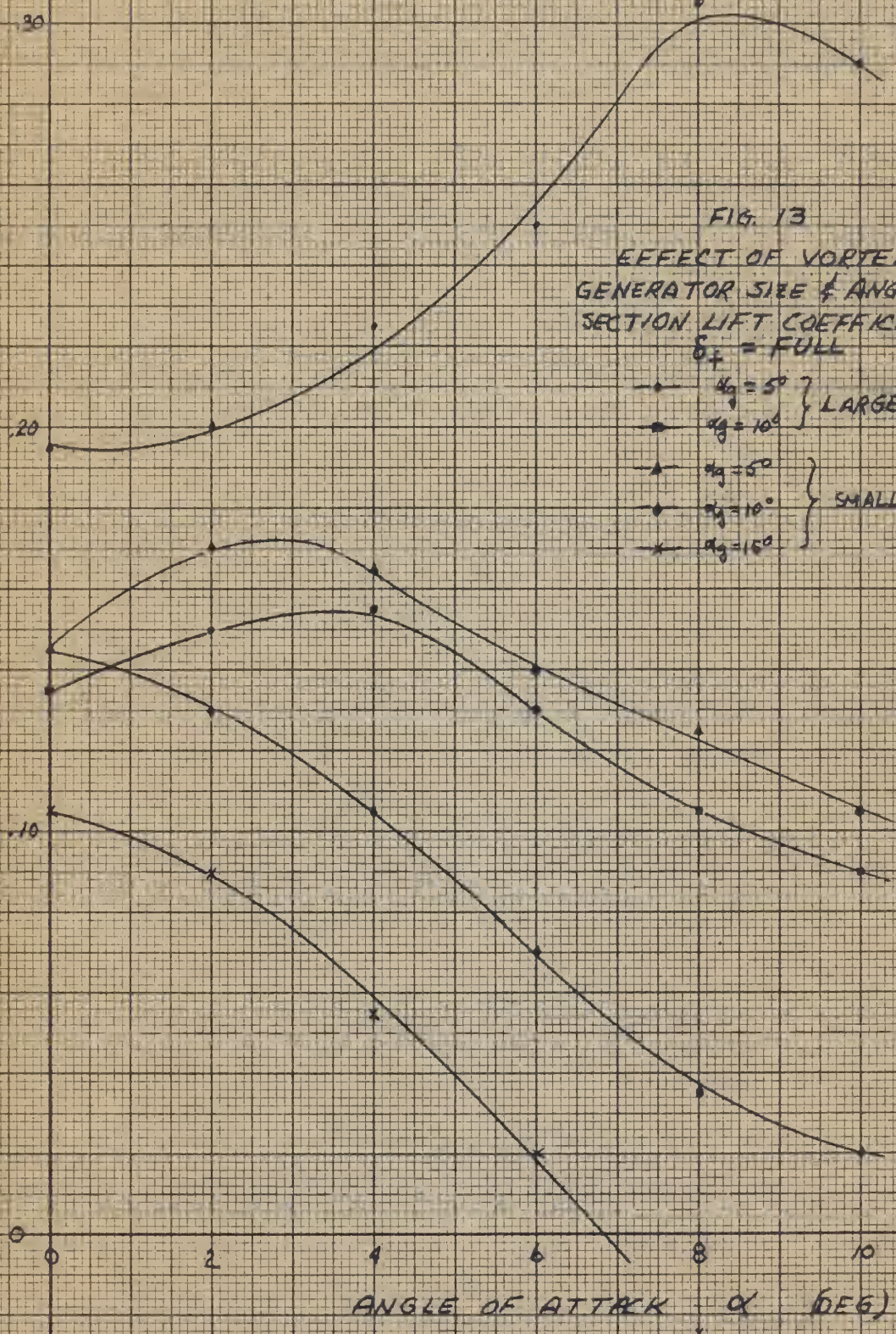
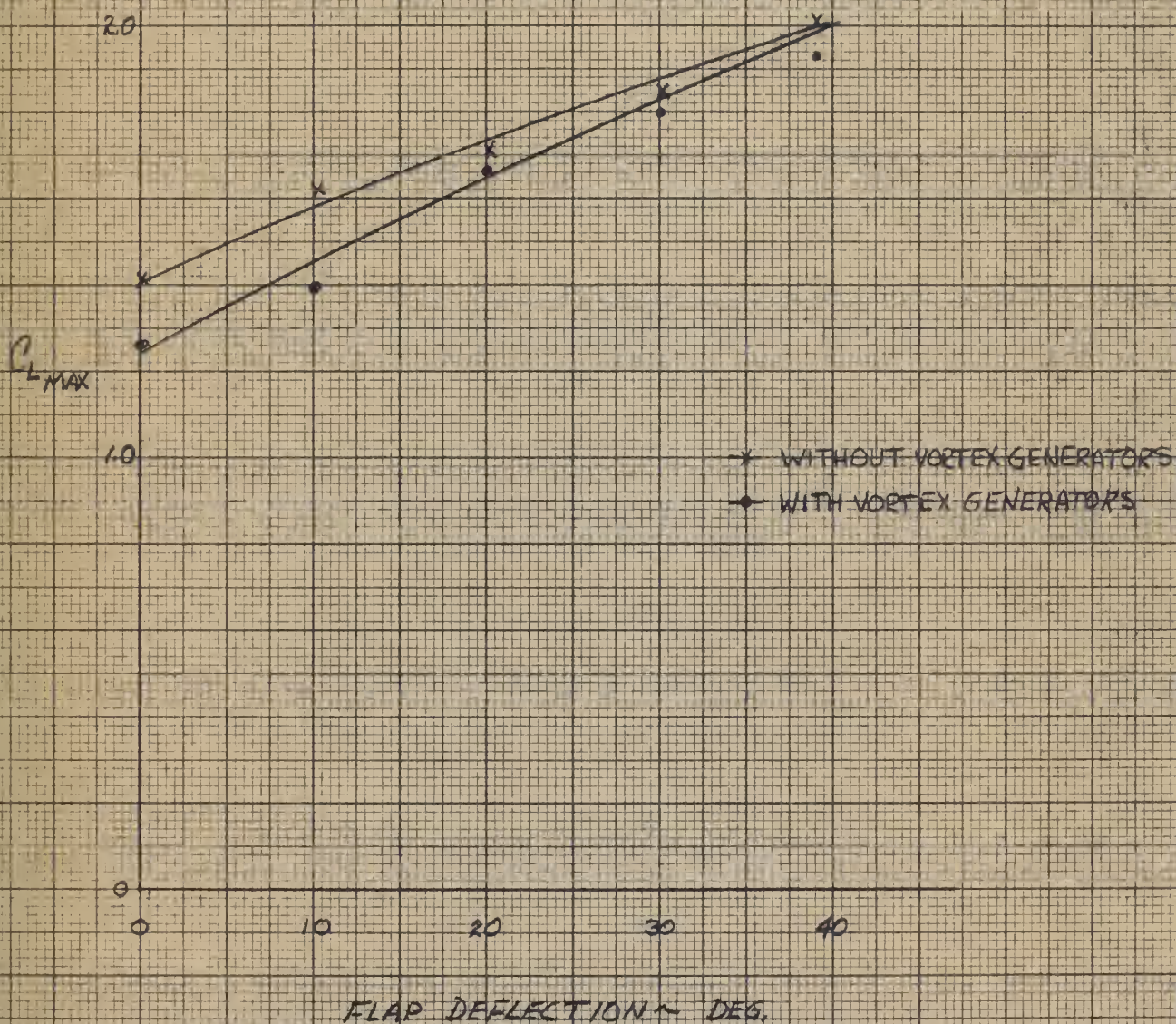






FIG. 14  
 $C_{L\text{MAX}}$  VS FLAP DEFLECTION  
POWER OFF  
NAVION NS113K







MAXIMUM LIFT COEFFICIENT -  $C_{L_{max}}$

$\delta_1 = \text{FULL}$

$\delta_1 = 1/2$

$\delta_1 = \text{ZERO}$

FIG. 15

$C_{L_{max}}$  VS POWER REQUIRED  
LEVEL FLIGHT  
SEA LEVEL, STANDARD DAY

○ WITHOUT VORTEX GENERATORS  
\* WITH VORTEX GENERATORS

BRAKE HORSEPOWER REQUIRED

100

90

80

70

60

50

40

14

12

10

2.0

1.8

1.6





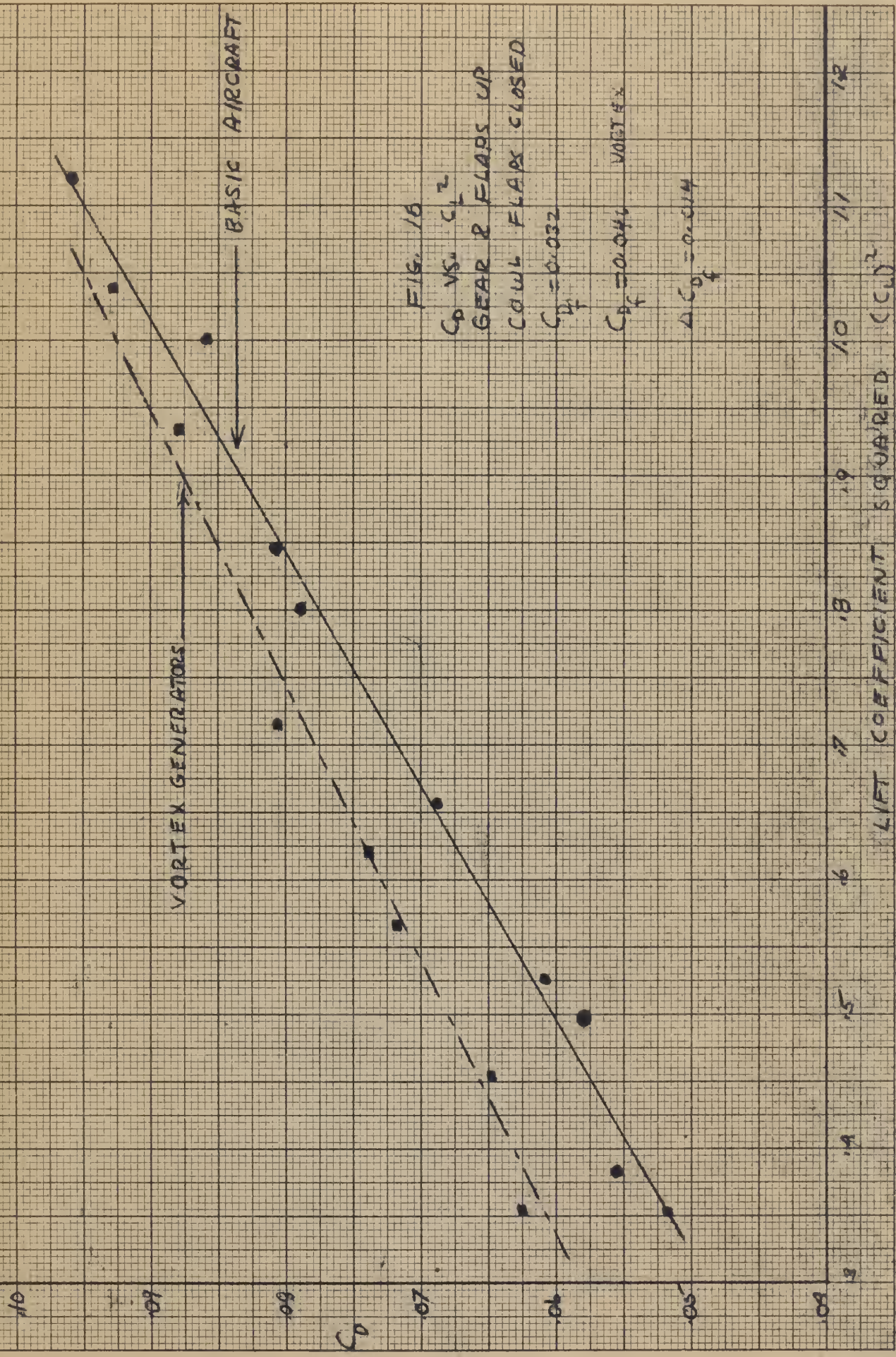


FIG. 16

$C_D$  VS.  $C_L^2$

GEAR & FLAPS UP

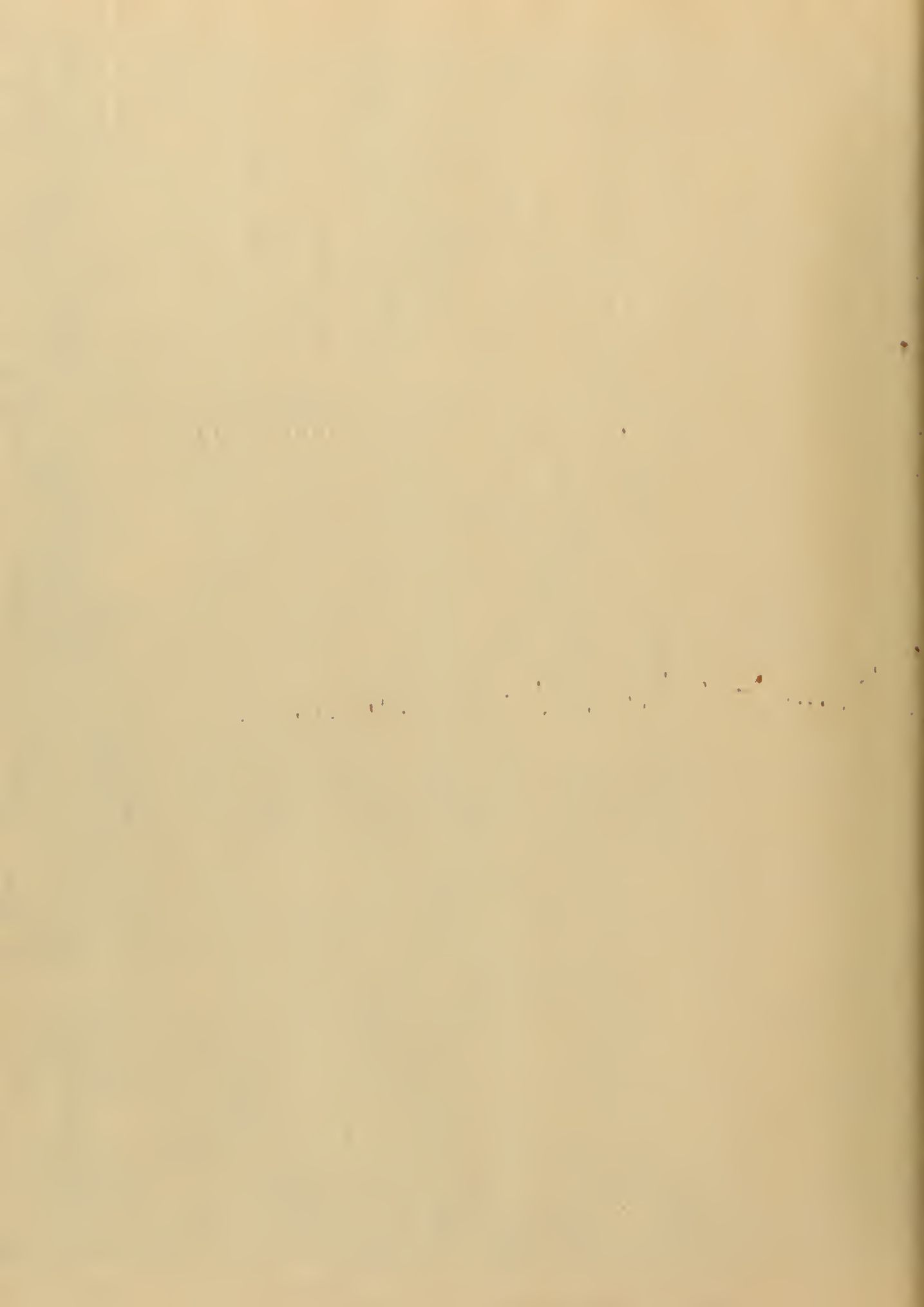
COWL FLAPS CLOSED

$C_{Df} = 0.032$

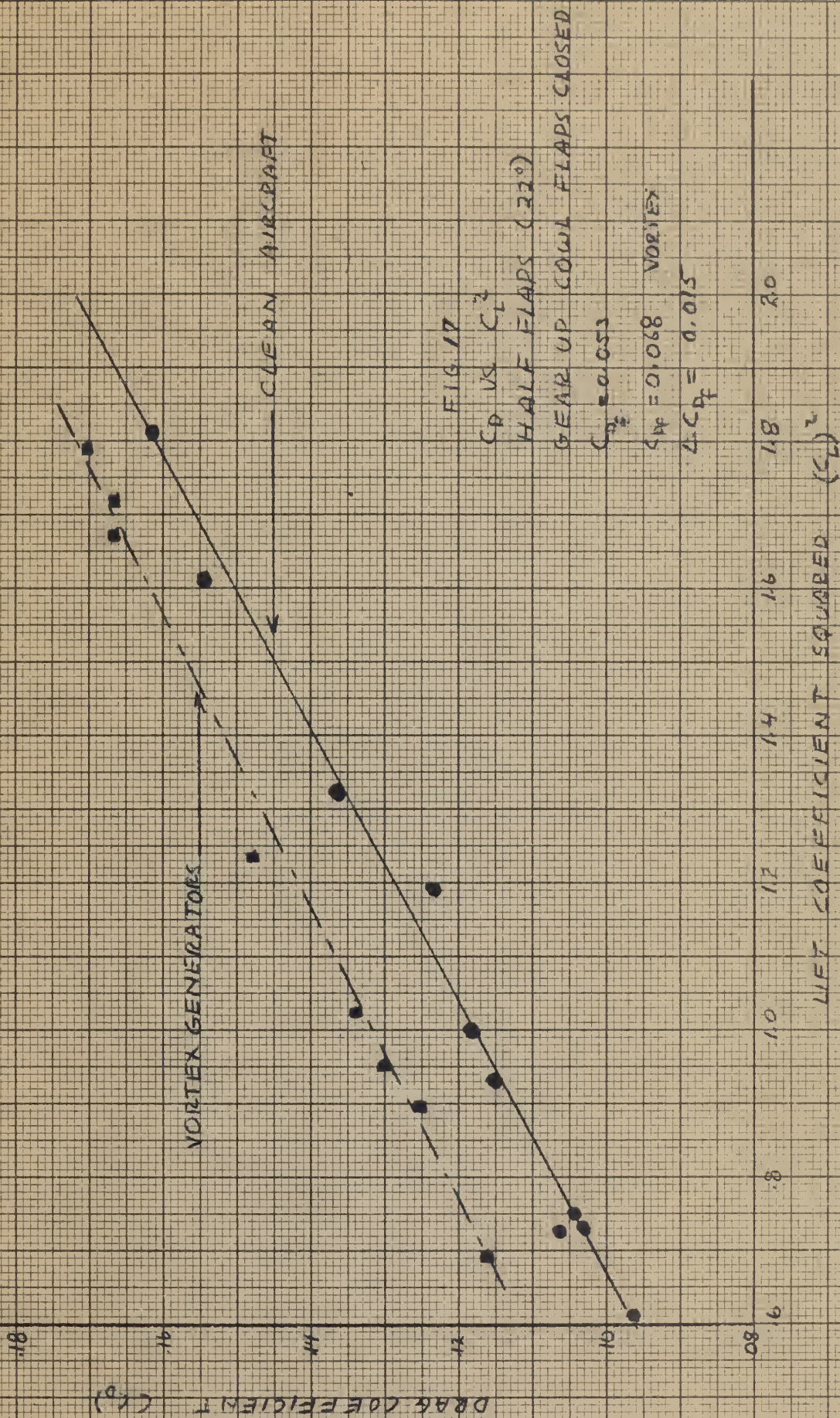
$C_{Df} = 0.046$  VORTEX

$\Delta C_{Df} = 0.014$

LIFT COEFFICIENT SQUARED ( $C_L^2$ )











DRA G COEFFICIENT ( $C_D$ )

22

20

18

16

14

12

LIFT COEFFICIENT SQUARED ( $C_L$ )<sup>2</sup>

5

7

9

11

13

15

17

19

21

CLEAN AIRCRAFT

VORTEX GENERATORS

FIG. 18

$C_D$  VS.  $C_L^2$

FULL FLAPS

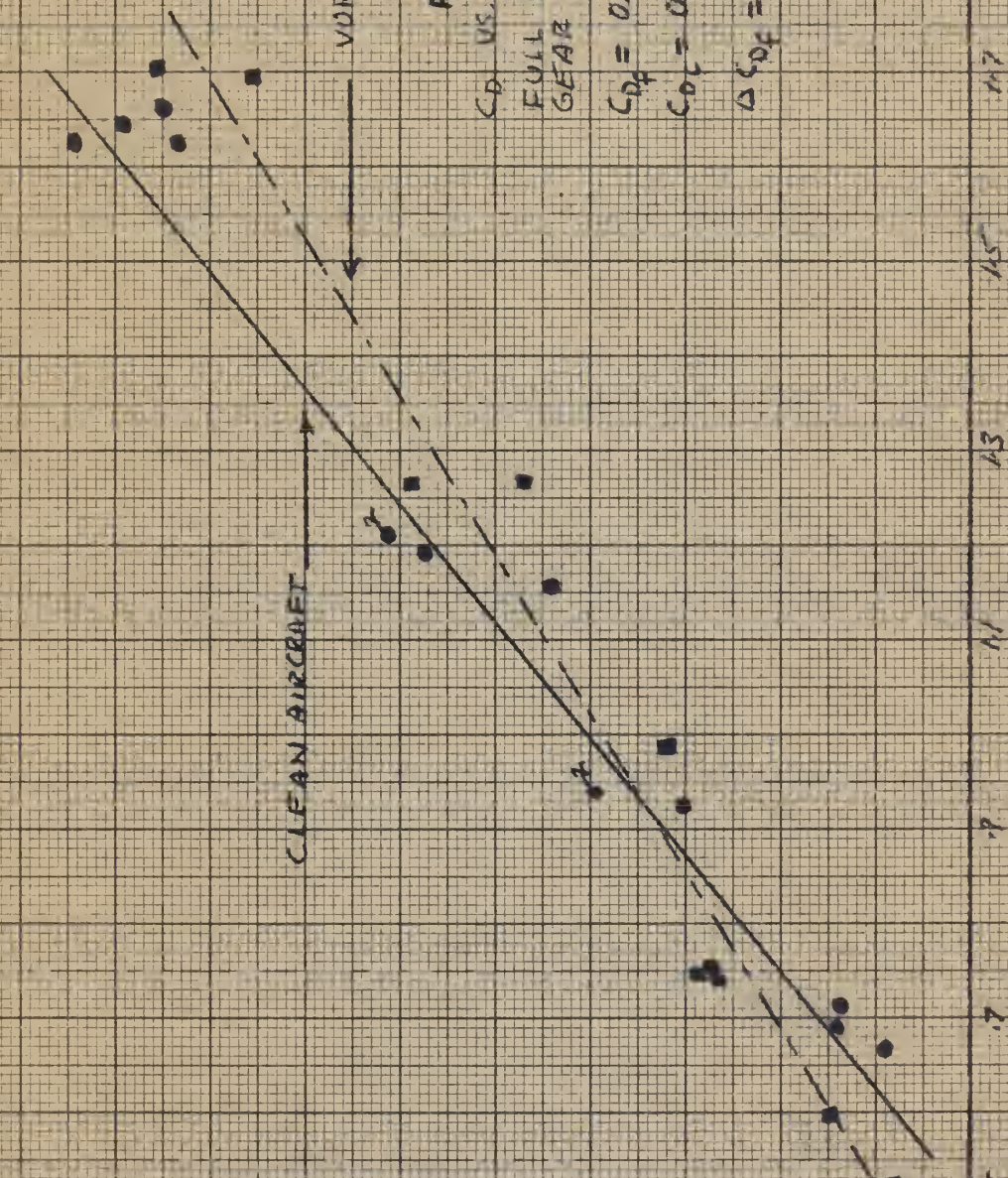
GEAR UP COWL FLAPS CLOSED

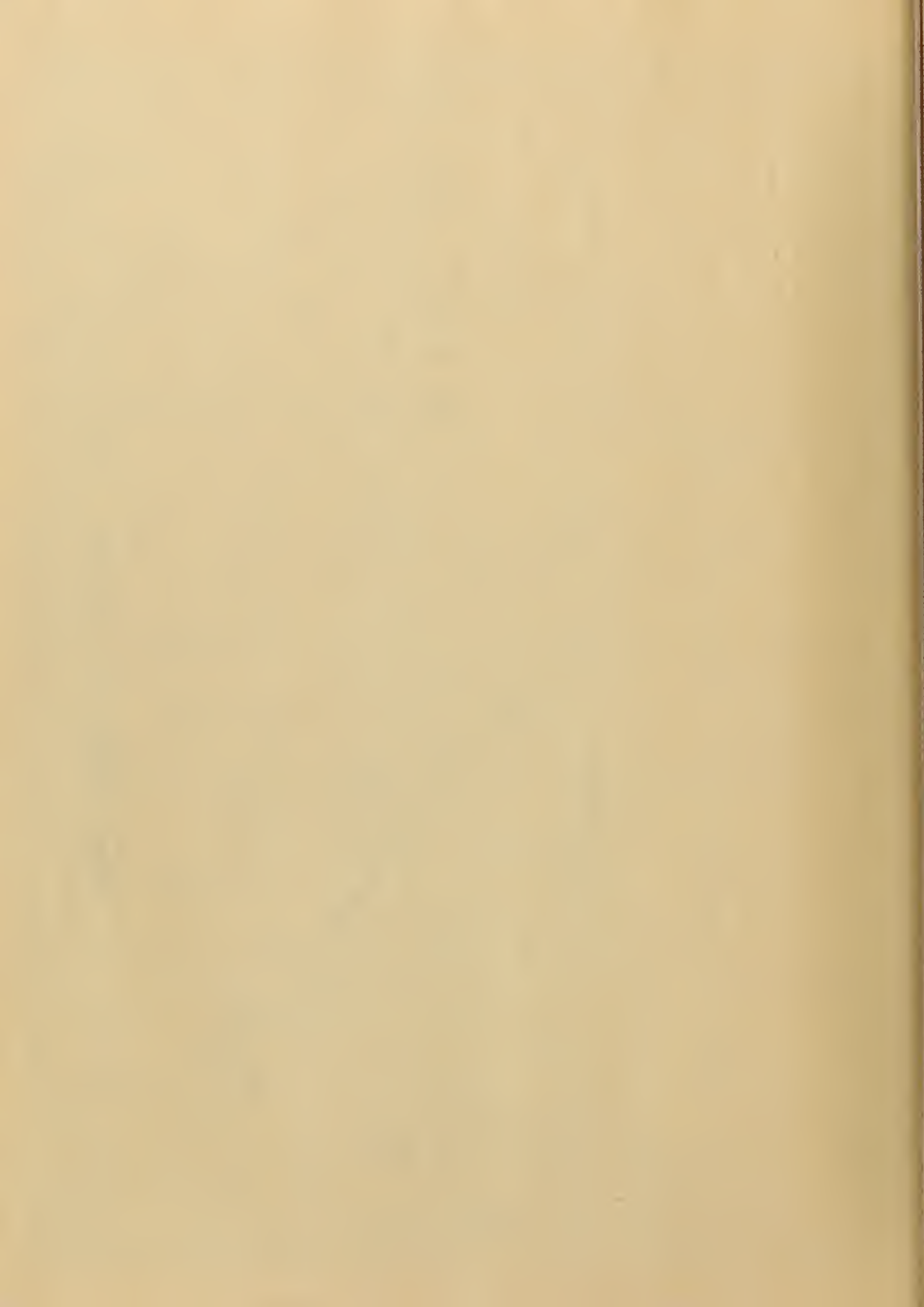
$C_{Df} = 0.072$

$C_{Di} = 0.09$

VORTEX

$\Delta C_{Df} = 0.018$







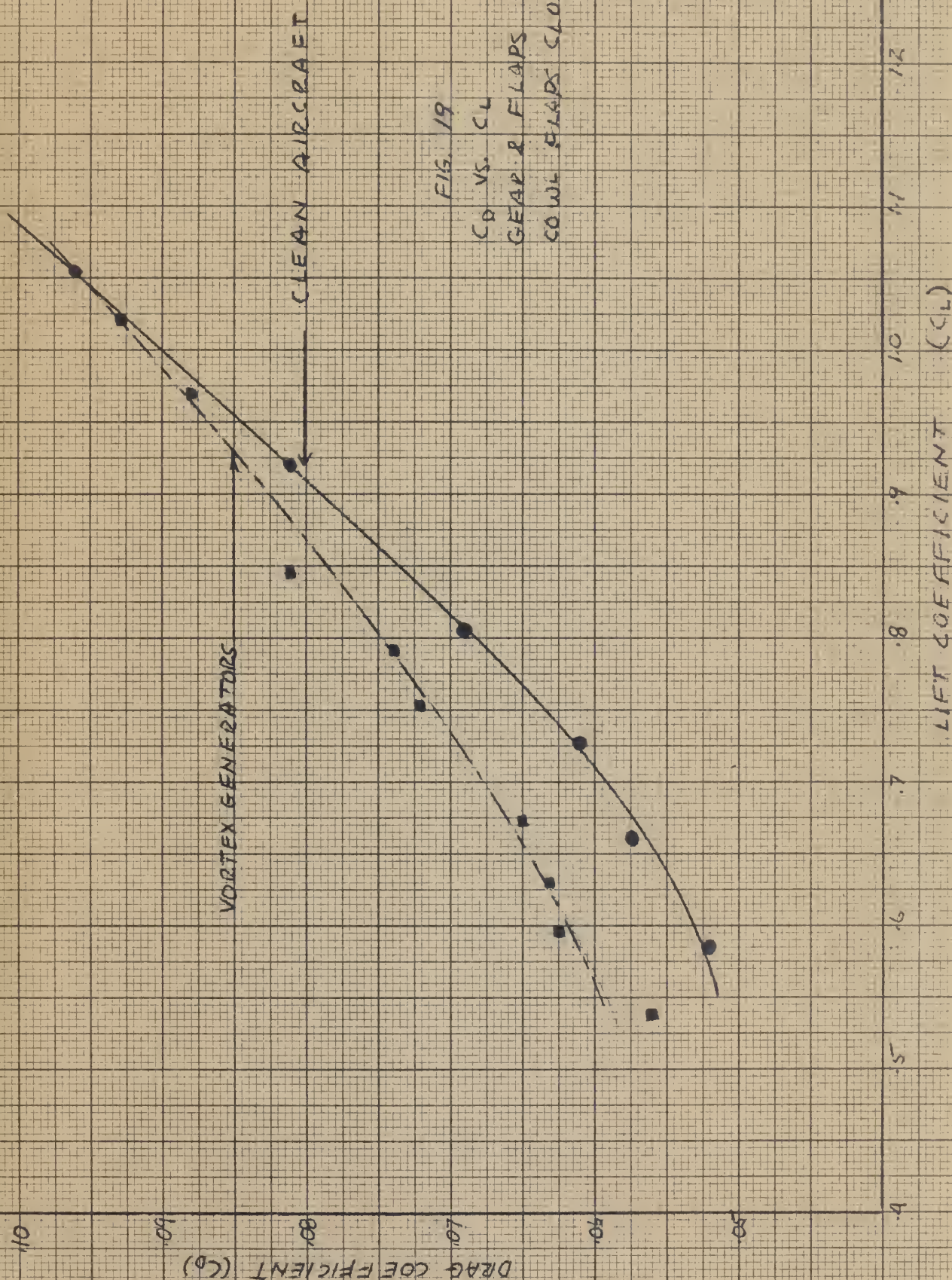
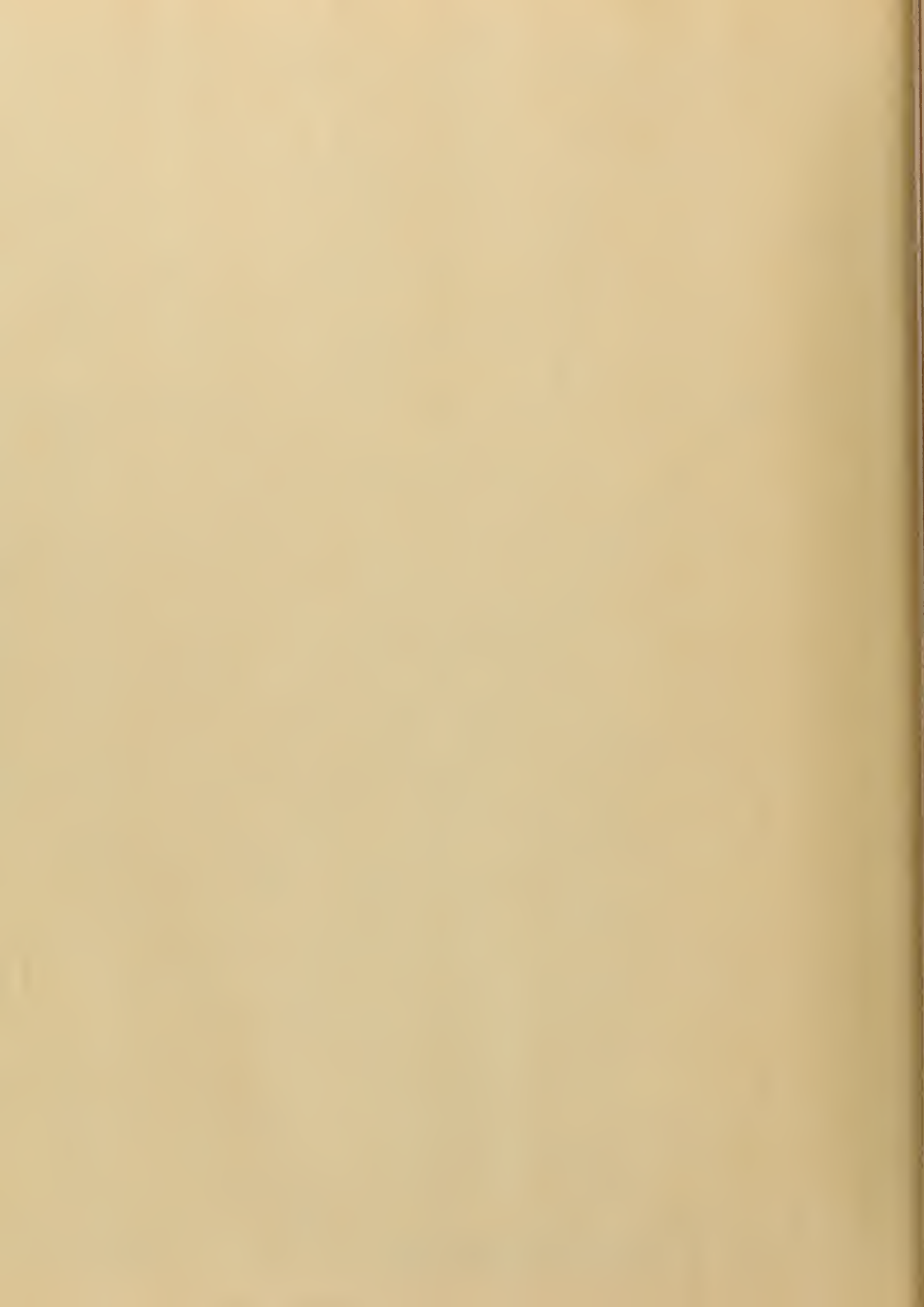


FIG. 19

$C_D$  VS.  $C_L$   
 GEAR & FLAPS UP  
 COW FLAPS CLOSED





DRAG COEFFICIENT ( $C_D$ )

LIFT COEFFICIENT ( $C_L$ )

VORTEX GENERATORS

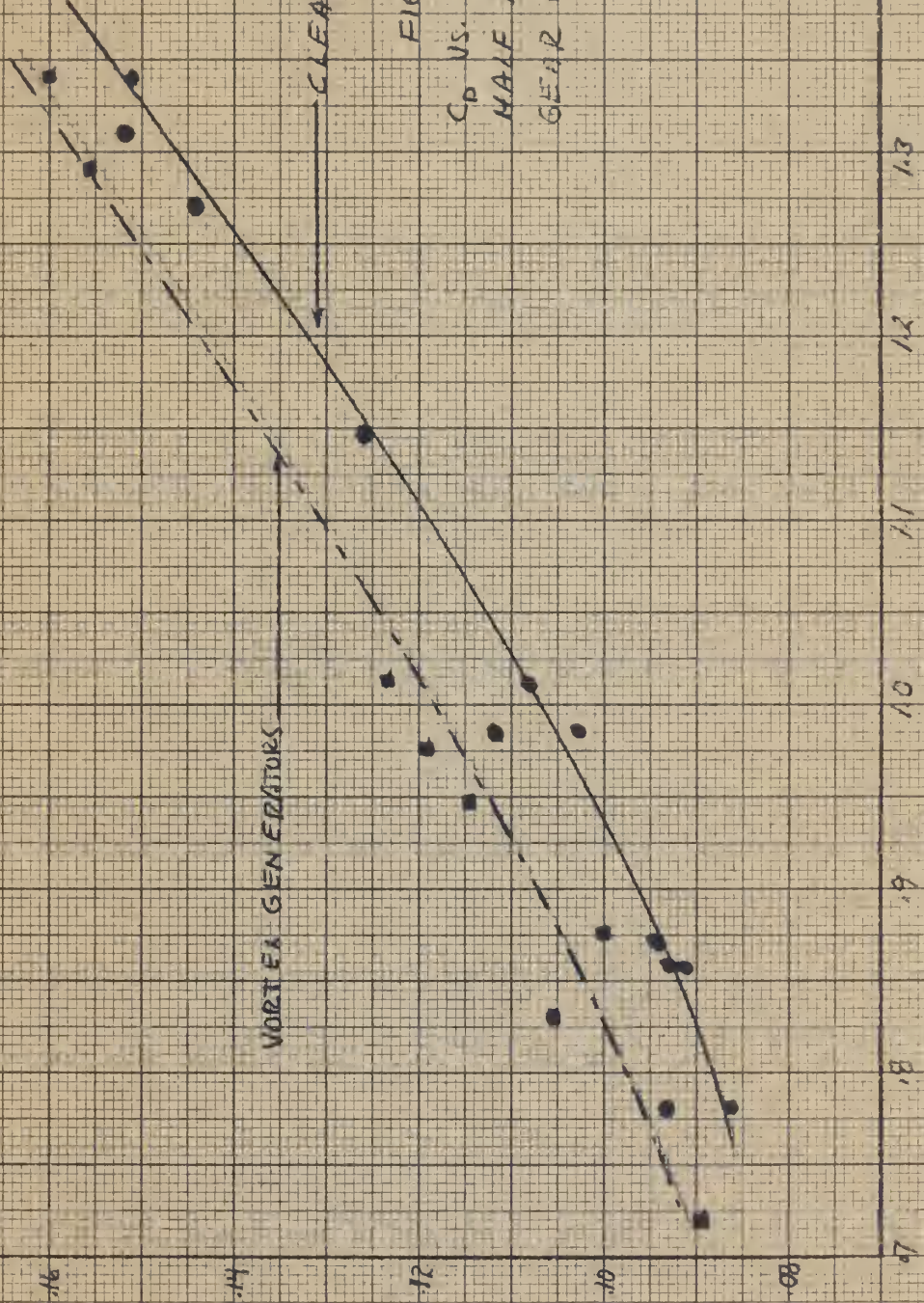
CLEAN AIRCRAFT

FIG. 20

$C_D$  VS.  $C_L$

HAIR FLAPS (22°)

GEAR UP COWL FLAPS CLOSED







22

20

18

16

14

12

DRAG COEFFICIENT ( $C_D$ )

0.7

0.8

0.9

1.0

1.1

1.2

1.3

1.4

1.5

LIFT COEFFICIENT ( $C_L$ )

CLEAN AIRCRAFT

VORTEX GENERATORS

FIG. 21

$C_D$  VS.  $C_L$   
FULL FLAPS  
COWL FLAPS CLOSED GEAR UP

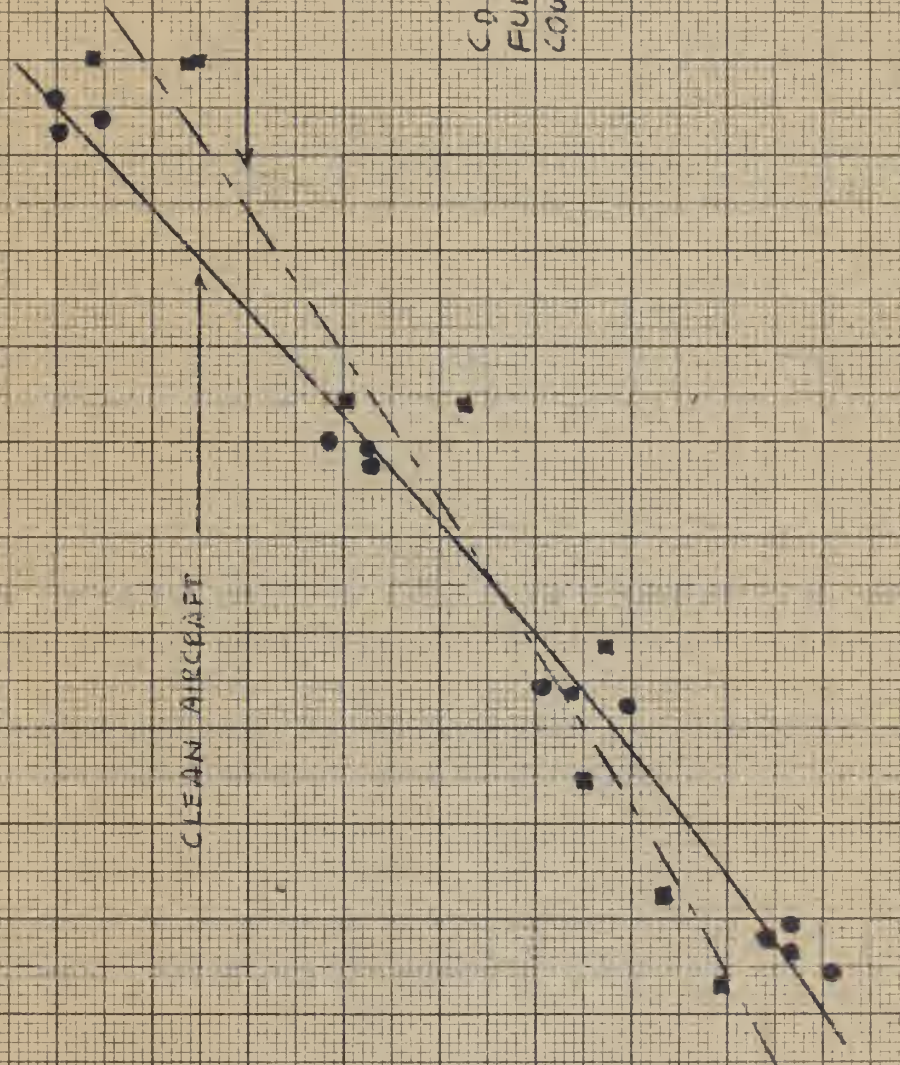






FIG. 22  
ELEVATOR ANGLE TO  
TRIM VS. INDICATED  
AIRSPEED  
ZERO FLAPS

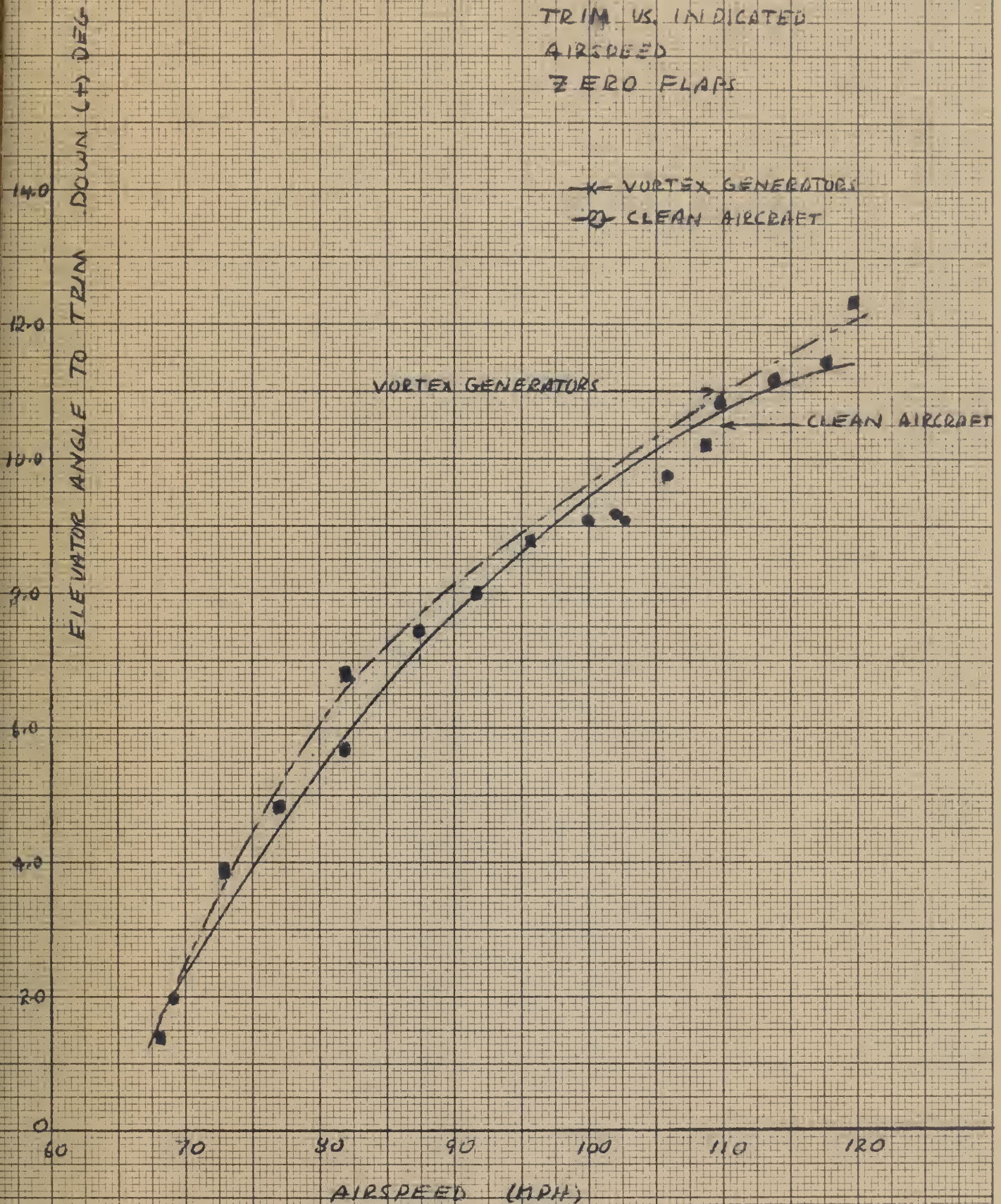






FIG. 23  
ELEVATOR ANGLE TO  
TRIM VS. INDICATED  
AIRSPEED  
HALF FLAPS

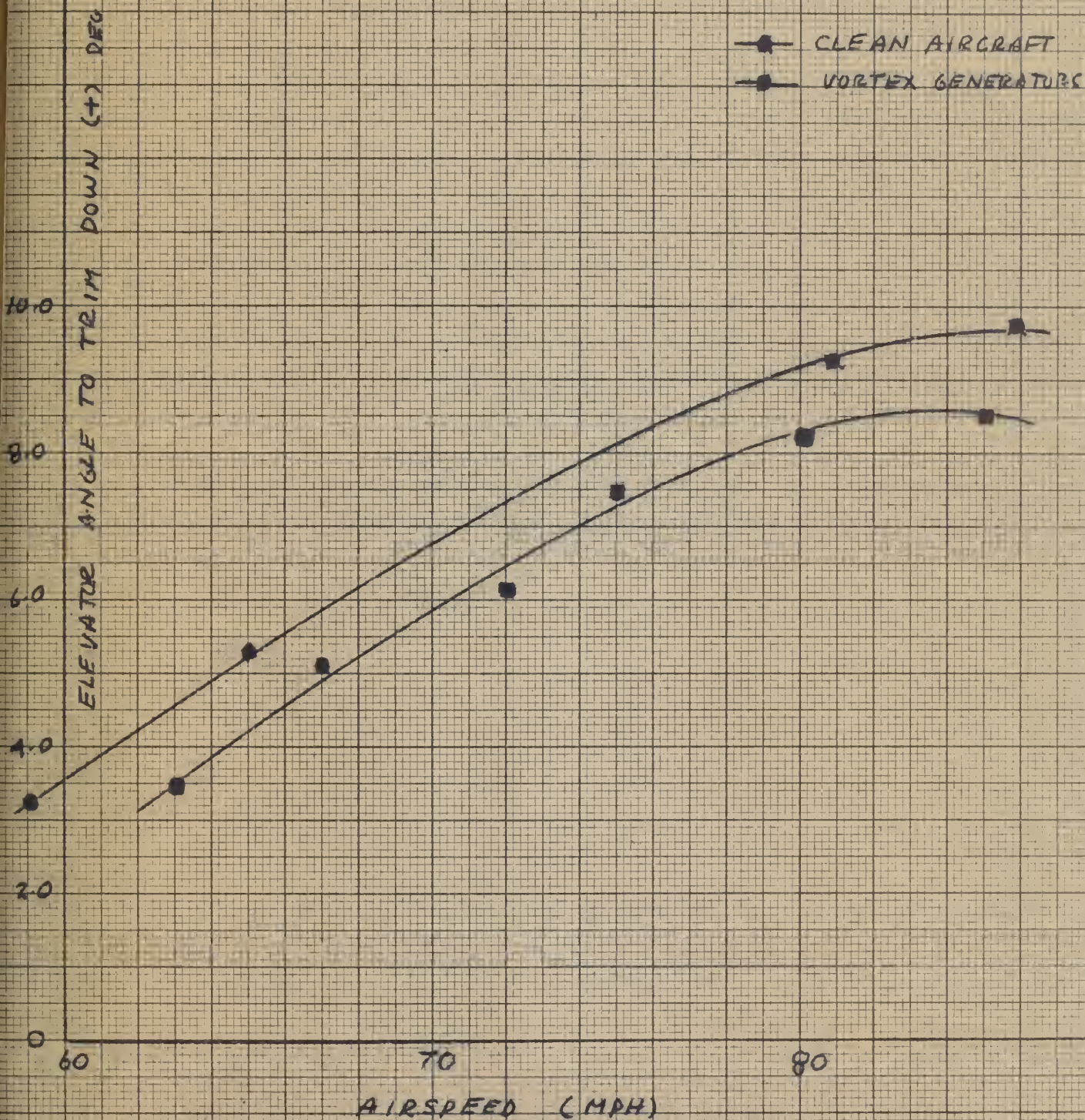






FIG 24  
ELEVATOR ANGLE TO  
TRIM VS.  
INDICATED AIRSPEED  
FULL FLAPS

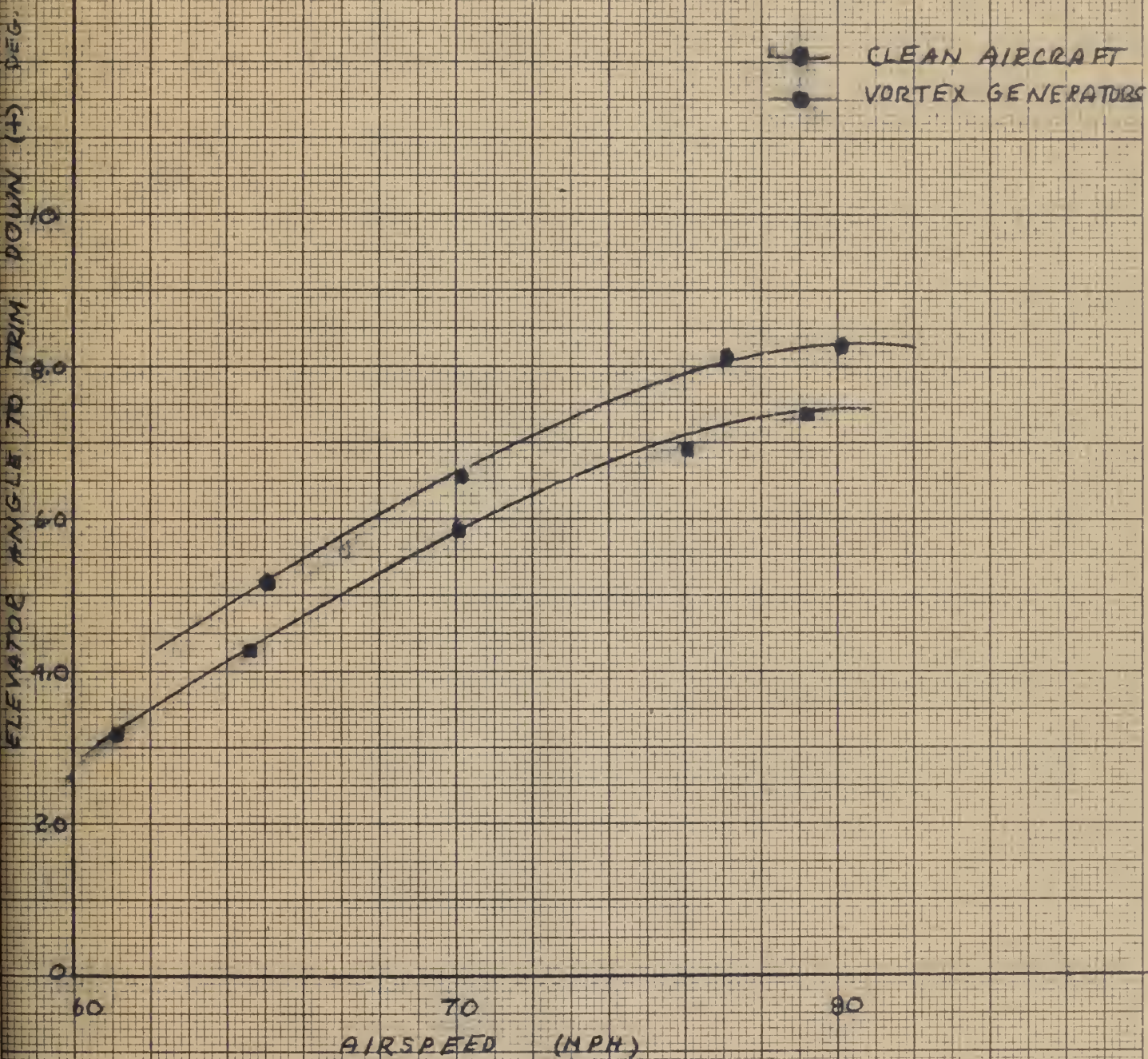






FIG. 25  
POWER REQUIRED FOR LEVEL FLIGHT

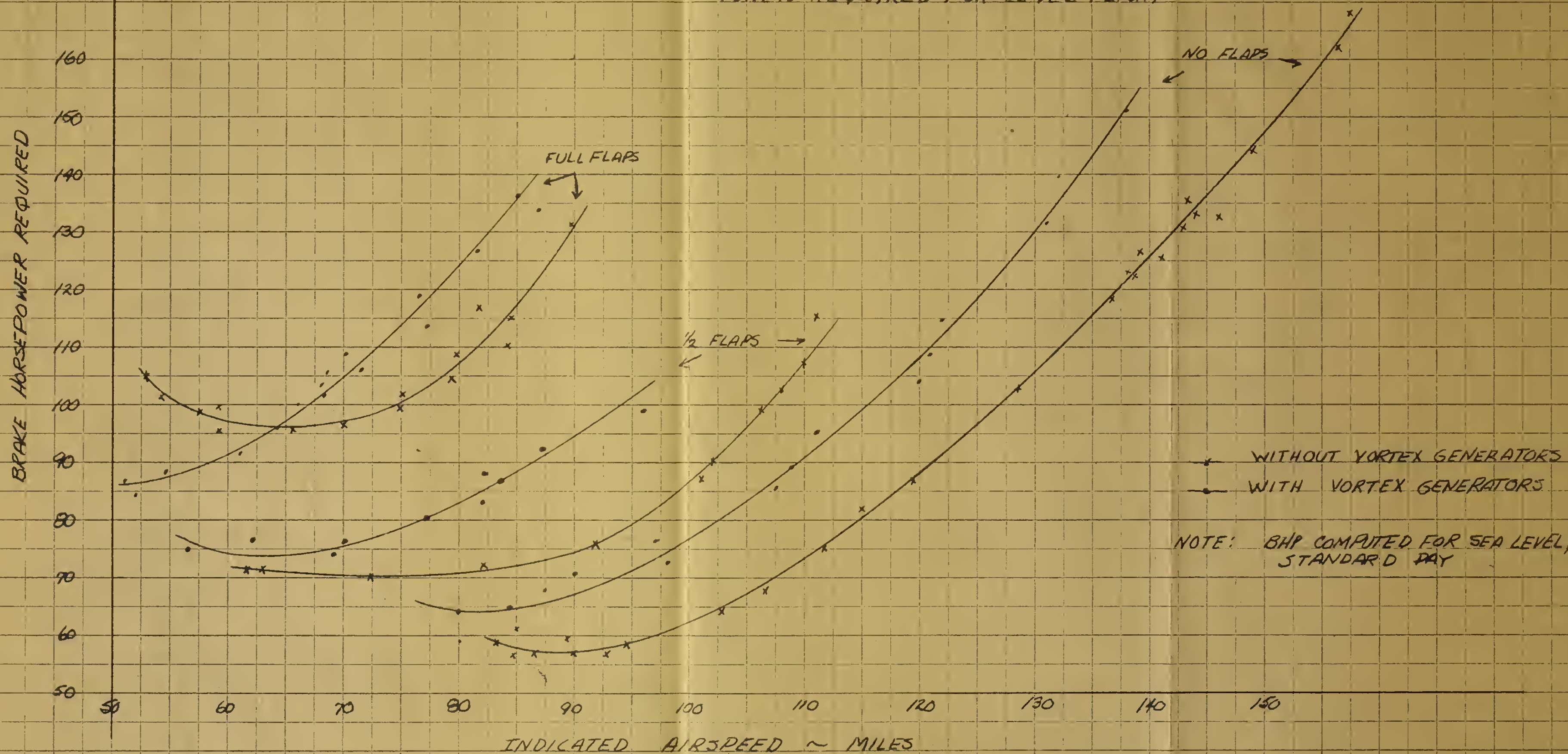






FIG. 26  
 $C_L$  VS  $\alpha_{FRL}$   
 NAVION N5113K

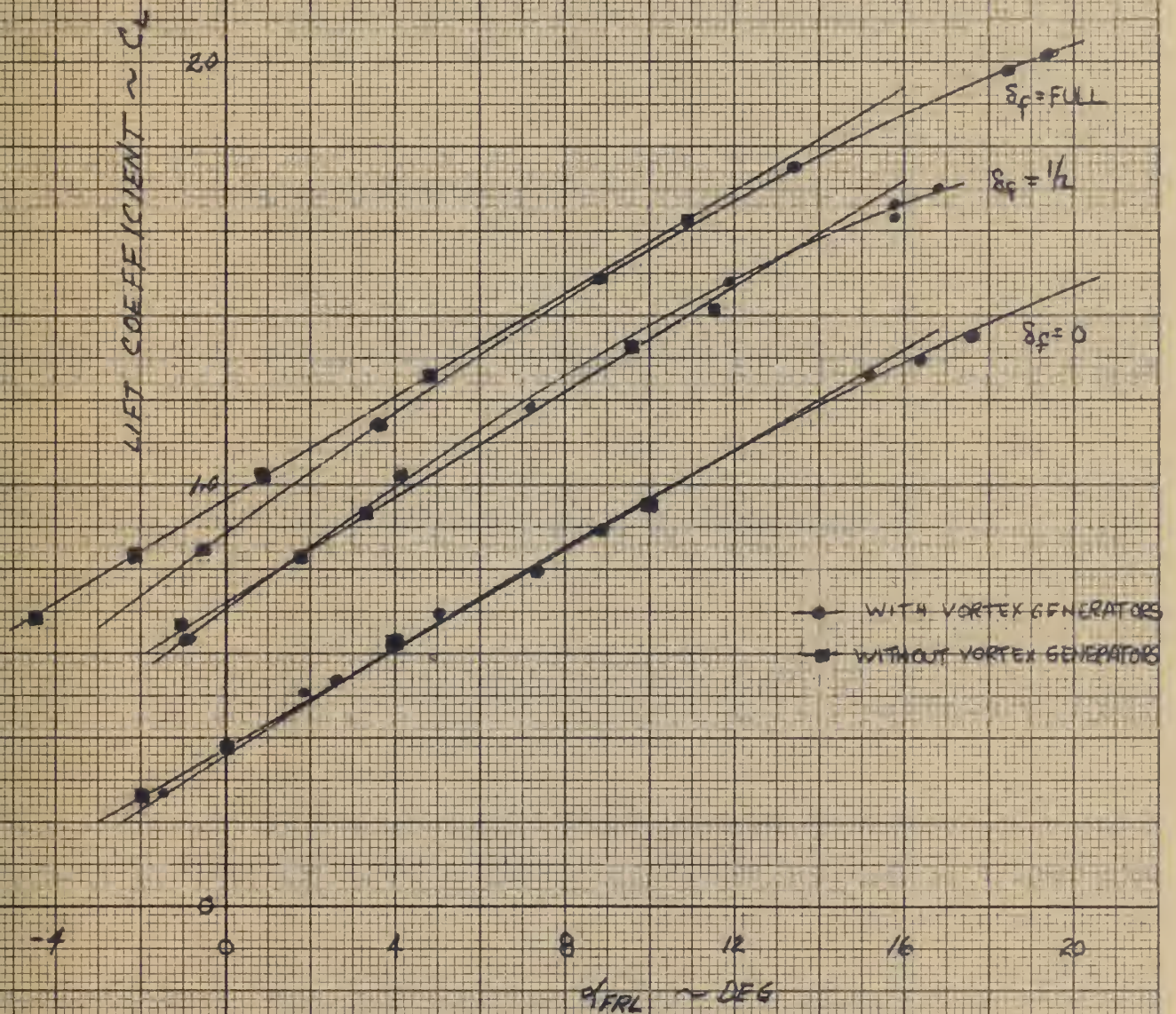




Fig. 27  
FLOW OVER FLAPS

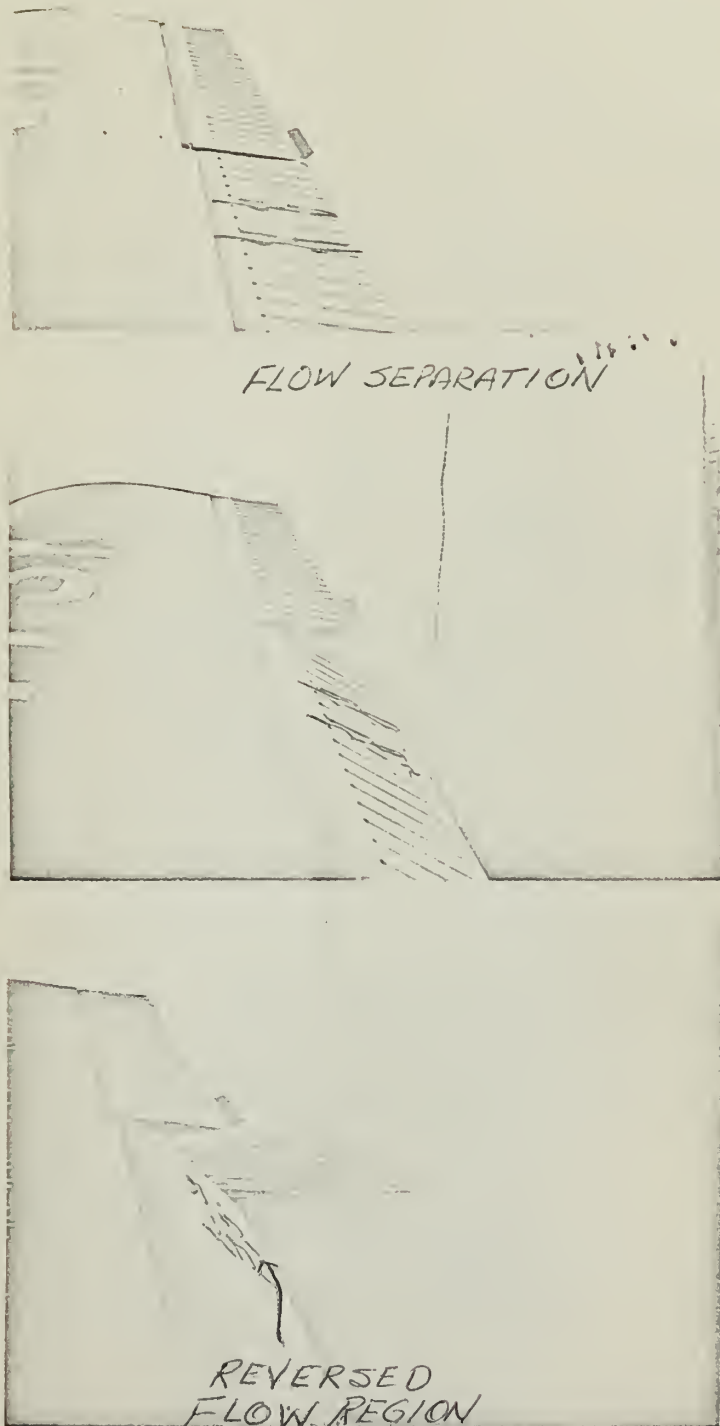
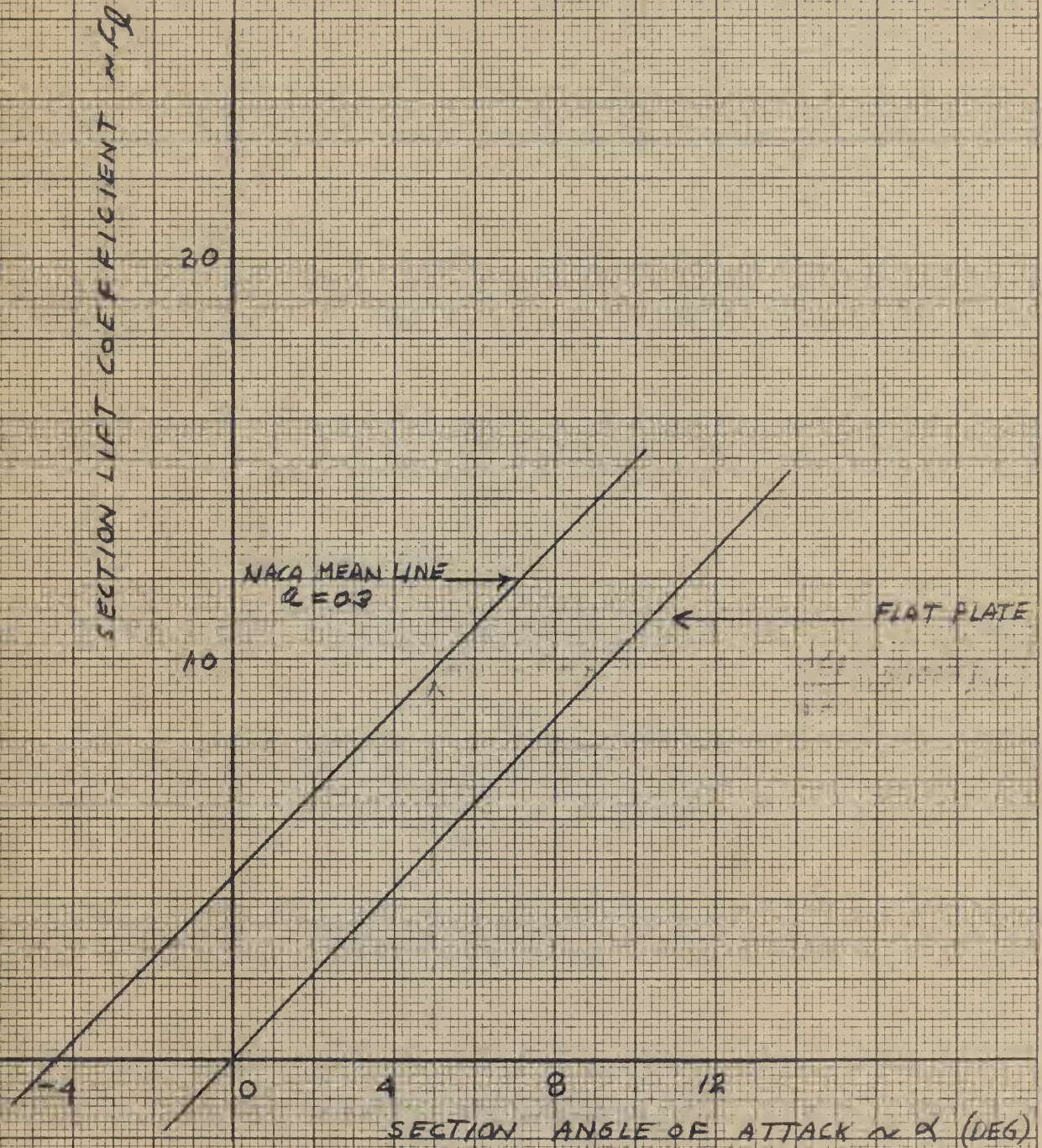


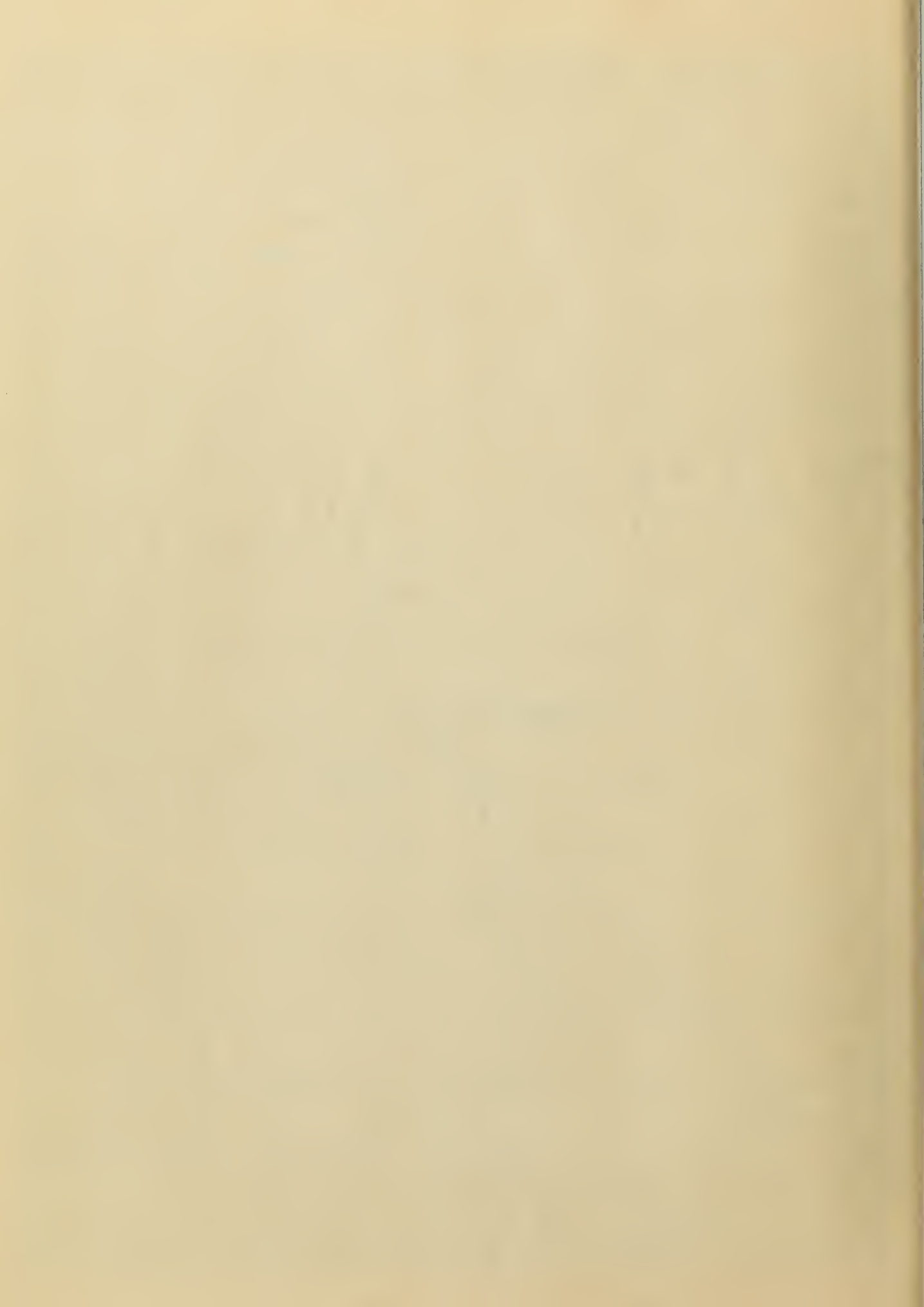






FIG. 28  
SECTION LIFT CURVES  
FOR A FLAT PLATE  
AND A NACA MEAN LINE  $q=0.3$













thesK49

An application of vortex generators to s



3 2768 002 10899 5

DUDLEY KNOX LIBRARY